Analytical Biochemistry xxx (xxxx) xxx

Contents lists available at ScienceDirect

Analytical Biochemistry

journal homepage: www.elsevier.com/locate/yabio

Aptasensors for mycotoxin detection: A review

Xhensila Shkembi [a], Marketa Svobodova [a], Vasso Skouridou [a], Abdulaziz S. Bashammakh [b], Abdulrahman O. Alyoubi [b], Ciara K. O'Sullivan [a,c,*]

[a] INTERFIBIO, Nanobiotechnology and Bioanalysis Group, Departament d'Enginyeria Química, Universitat Rovira i Virgili, Avinguda Països Catalans 26, 43007 Tarragona, Spain
[b] Department of Chemistry, Faculty of Science, King Abdulaziz University, P.O. Box 80203, 21589 Jeddah, Saudi Arabia
[c] Institució Catalana de Recerca i Estudis Avancats (ICREA), Passeig Lluís Companys 23, 08010 Barcelona, Spain

ARTICLE INFO

Keywords:
Patulin
T-2 toxin
Aflatoxin B1, B2
Zearalenone
Fumonisin B1
Ochratoxin

ABSTRACT

Mycotoxins are toxic compounds produced by fungi, which represent a risk to the food and feed supply chain, having an impact on health and economies. A high percentage of feed samples have been reported to be contaminated with more than one type of mycotoxin. Systematic, cost-effective and simple tools for testing are critical to achieve a rapid and accurate screening of food and feed quality. In this review, we describe the various aptamers that have been selected against mycotoxins and their incorporation into optical and electrochemical aptasensors, outlining the strategies exploited, highlighting the advantages and disadvantages of each approach. The review also discusses the different materials used and the immobilization methods employed, with the aim of achieving the highest sensitivity and selectivity.

1. Introduction

The Food and Agriculture Organization (FAO) of the United Nations states that nearly 25% of food produced in the world is affected by toxigenic fungi, leading to mycotoxins entering the food chain. Mycotoxins are secondary metabolite produced by fungus, that colonize on crops either during harvesting or during storage, and the word mycotoxin originates from the Greek word "mukos" meaning fungus and the latin word "toxicum" referring to poison [1].

There are five mycotoxin groups that are frequently found in food: (i) deoxynivalenol/nivalenol, (ii) zearalenone, (iii) ochratoxin, (iv) fumonisins and (v) aflatoxins. The food-borne mycotoxins with the greatest significance for human health in tropical developing countries are the fumonisins and aflatoxins. Globally, mycotoxins have a significant impact on human and animal health, economies and international trade [2–6]. Despite efforts to control fungal infection, extensive mycotoxin contamination has been reported to occur in feed and food. Mycotoxin contamination of feed is an area of great concern due to the negative health effects on animals. Furthermore, according to the amount present and risk of each toxin, feed contamination can also represent a hazard for the safety of food of animal origin and contribute to mycotoxin intake in humans [7]. Recent surveys have been carried out to evaluate the incidence of mycotoxin contamination [8,9]. On a global level, 30%–100% of food and feed samples are co-contaminated [10–14], and 300 mycotoxins have been identified and reported. Among them, the most important are: aflatoxins (AF), ochratoxins (OTA), fumonisin, patulin, zearalenone (ZEN), and trichothecenes including deoxynivalenol (DON) and T-2 toxin [15,16]. In order to ensure the food safety against mycotoxin, sensitive and reliable determination strategies are required [17].

There is a continuous increase in the number of mycotoxins, and there are only assays/kits/rapid tests available for a handful of the numerous harmful mycotoxins. To date, none of the rapid tests can differentiate between the types of aflatoxins (*e.g.* B1, B2, M1, G1, G2), ochratoxins (A, B, C) and fumonisins (B1, B2, B3)). There have been many efforts to develop methods for mycotoxin determination, based on lab-dependent methods and lab-independent methods [18–20]. For lab-dependent methods, typically, high performance liquid chromatography and gas chromatography, along with fluorescent detectors or mass spectrometry detectors have been reported [21,22]. These lab-dependent methods have the advantages of high sensitivity and stability, while having disadvantages of the high cost of equipment, labor, time and the inherent requirement to carry out the assay in a centralized laboratory, and it is desirable to have assays that are suitable for on-site monitoring of the mycotoxin risk in food. Among several

* Corresponding author. INTERFIBIO, Nanotechnology and Bioanalysis Group, Departament d'Enginyeria Química, Universitat Rovira i Virgili, Avinguda Països Catalans 26, 43007 Tarragona, Spain.
E-mail address: ciara.osullivan@urv.cat (C.K. O'Sullivan).

https://doi.org/10.1016/j.ab.2021.114156
Received 16 November 2020; Received in revised form 10 February 2021; Accepted 4 March 2021
Available online 11 March 2021
0003-2697/

Abbreviations

Deoxynivalenol DON
Zearalenone ZEN
Ochratoxin OTA
Fumonisins FB1/FB2/FB3
Aflatoxin AF B1/B2/M1/G1/G2
Patulin PAT
T-2 toxin T-2
Electrochemical impedance spectroscopy EIS
Surface-enhanced Raman spectroscopy SERS
Surface Plasmon Resonance SPR
Systematic evolution of ligand by exponential enrichment SELEX
Single-strand DNA ssDNA
Lateral flow LF
High performance liquid chromatography HPLC
Gas chromatography GC
Graphene oxide GO
Graphene oxide SELEX GO-SELEX
ZnO nanorods ZnO-NRs
Polyethylene glycol PEG
Screen-printed carbon electrodes SPCEs
Fluorescence resonance energy transfer FRET
Fluorescein amidites FAM
Carboxytetramethylrhodamine TAMRA
European Food Safety Authority EFSA
Ultra-performance liquid chromatography−tandem mass spectrometry UPLC−MS/MS
Gas chromatography−tandem mass spectrometry GC−MS/MS
Liquid chromatography tandem mass spectrometry LC-MS-MS
Carbon electrode GCE
Molybdenum disulfide-polyaniline-chitosan-gold nanoparticles MoS_2-PANI-Chi-Au
Reduced graphene oxide-tetraethylene pentamine-gold@platinum nanorods rGO-TEPA-Au@Pt NRs
Aptamer functionalized silver nanoclusters apt-AgNCs
Molybdenum disulfide MoS_2
Reduced graphene oxide/molybdenum disulfide/polyaniline@gold nanoparticles (RGO/MoS_2/PANI@AuNPs/Apt)
Aptamer-incorporated tetrahedral DNA nanostructures TDNs
Amino-terminated aptamer conjugated magnetic-bead (CS–Fe_3O_4)
Gold nanotriangles GNTs
Magnetic solid-phase extraction MSPE
Coated magnetic agarose microspheres MAMs
Enzyme-linked immunosorbent assay ELISA
Enzyme-linked oligonucleotide assay ELONA
Quantitative reverse transcription PCR RT-qPCR
Polymerase chain reaction PCR
Glassy carbon electrode GCE
Reduced molybdenum disulfide $rMoS_2$
Silica photonic crystal microsphere SPCM

lab-independent determination methods, antibody or aptamer based sensors have garnered increasing attention due their advantages of high sensitivity and specificity, high throughput, portability and reusability [23–25]. Whilst microfluidic devices and microarrays offer the possibility of in situ detection, lateral flow assays are the most attractive in terms of cost, simplicity of use and do not need any type of reader device [26].

The purpose of this review is to highlight the recent developments of aptamers against different mycotoxins and their use in a range of nanomaterial-based electrochemical and optical aptasensors, including detection using electrochemical impedance spectroscopy (EIS) [27], surface-enhanced Raman spectroscopy (SERS) [28] or lateral flow (LF) [29].

Aptamers are single-stranded DNA or RNA molecules that can bind to

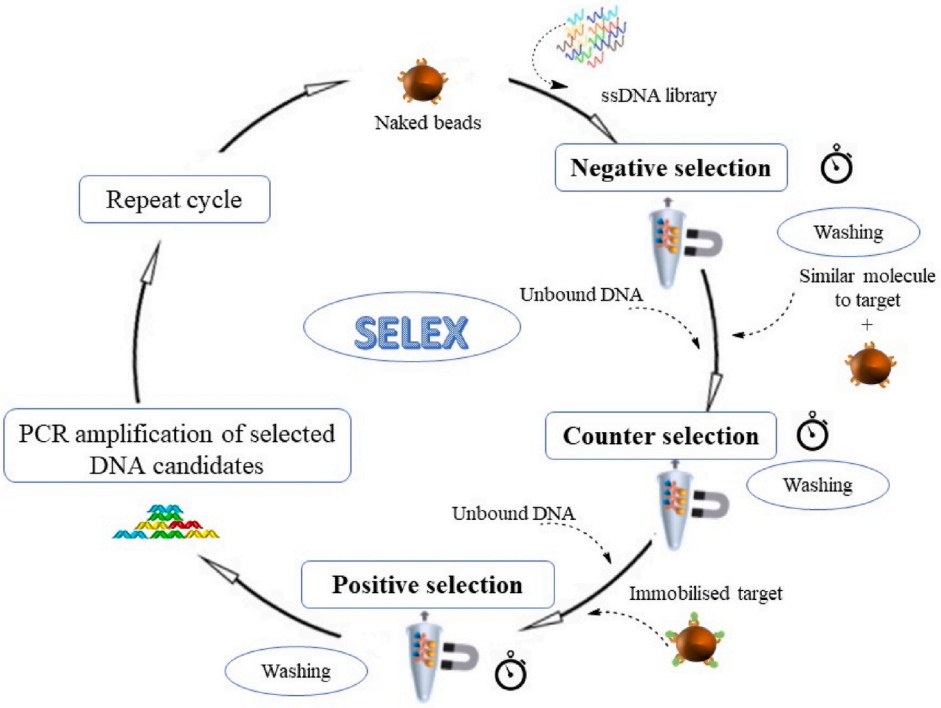

Fig. 1. Schematic representation of SELEX process.

pre-selected targets through a repetitive process termed systematic evolution of ligand by exponential enrichment (SELEX). SELEX was first described by Tuerk et al. [30] and was developed for the identification and separation of aptamers with specific properties through *in vitro* screening from random libraries [31]. As can be seen in Fig. 1, traditional SELEX consists of steps of incubation, separation, dissociation, and PCR amplification. Generally, high affinity, selective aptamer sequences can be obtained after 8–20 rounds of enrichment. Since its inception, SELEX has evolved considerably, and current SELEX technologies include negative screening, counter screening, and automated technologies. In order to remove non-specific binders, and increase the aptamer specificity, negative and counter selection are used before the positive selection when the target molecule is introduced. Negative selection is selection against non-target components, present in the buffer selection or in the unmodified matrix (e.g naked beads), whilst counter selection is performed against molecules that are structurally similar to the target or that can be found in the same sample or environment [32–34]. In comparison to antibodies aptamers can have a longer shelf life, are chemically stable, are robust even at elevated temperatures and their thermal denaturation is reversible [35]. Aptamers can be selected against toxic compounds and non-immunogenic compounds [36]. Due to their small size, aptamers can infiltrate tissues and cells, and are non-toxic and non-immunogenic [36–38]. Table 2 outlines the properties of the aptamers referred to in this review. Specifically detailing their structures, length and GC content. The cost of an aptamer, once selected, is considerably lower than antibodies, as they are produced by automated DNA synthesizers. The development of an aptamer-based test for the quantitative determination of mycotoxin in food samples could facilitate dynamic testing of agricultural products.

2. Mycotoxins and detection strategies

2.1. Patulin

Patulin (PAT) is a secondary metabolite of some fungi belonging to species of *Penicillium, Aspergillus,* and *Byssochlamys* [39]. It is a widespread contaminant of human foodstuffs, including fruits (apples, haws, tomatoes, pears) and nuts (almonds, hazelnuts, peanuts, and their products). Patulin has acute and chronic toxic effects on animal and human health. Acute toxicity is characterized by convulsions, lung, intestinal, liver bleeding and kidney damage. The chronic toxicity includes neurotoxicity, immunotoxicity, genotoxicity, teratogenicity, and possible carcinogenicity [40]. Until recently, the estimation of trace amounts was determined by chromatographic techniques [41], such as thin layer chromatography, high performance liquid chromatography (HPLC), gas chromatography (GC), and liquid chromatography tandem mass spectrometry (LC-MS-MS) [42–46]. Despite their accuracy, these methods are expensive, time-consuming and require qualified personnel. There is a mature need for portable devices for use at the point-of-need.

Graphene oxide (GO), chemically exfoliated from oxidized graphite, is considered as a promising material for signal enhancement in sensing. Due to its material properties, GO is ideal for the immobilization of various bio-recognition elements, including enzyme, aptamers and antibodies [47,48]. Exploiting specific properties such the ability of GO to quench fluorescence, its high conductivity, high mechanical and chemical strength [49,50], several GO based optical and electrochemical aptasensors have been developed for the detection of mycotoxins.

A successful aptamer against PAT was selected by Shijia Wu et al. [51] using GO-SELEX. This novel approach was firstly described by Park et al. [52] who selected an aptamer against Nampt protein. In principle, oligonucleotides are bound to the GO surface through $\pi-\pi$ stacking interactions between the nucleobases and sp^2 atoms of GO. In this approach, the nucleic acids of a random library adsorb on GO and when the target is introduced, it can induce a conformational change in nucleic acid sequences that have affinity against the target, thus releasing the aptamer from GO. The aptamers obtained via desorption are extracted, amplified, and proceed to the next round of SELEX. Adapting this new technique, an aptamer of 40 nucleotides was selected against patulin with high affinity and selectivity, with a dissociation constant (K_d) of 21.83 ± 5.022 nM. The selected aptamer was subsequently used as a recognition element to develop a detection method for patulin based on an enzyme-chromogenic substrate system. The colorimetric aptasensor exhibited a linear range from 50 to 2500 pg/mL, and the limit of detection was found to be 48 ng/L.

Baoshan et al. [53] describe an aptamer based assay using a gold electrode modified with a composite made from ZnO nanorods (ZnO-NRs) and chitosan. This design was exploited to increase the loading of AuNPs and aptamers on the electrode surface, effectively improving the detection performance of the electrode. The PAT concentration was determined by the change of the peak current (ΔI) of the redox probe $[Fe(CN)_6]$ after PAT incubation. The results displayed excellent sensitivity and a detection limit of 0.27 ng/L was achieved. Furthermore, the aptamer sensor was successfully applied to the detection of PAT in apple juice samples with a recovery of 95.6–104.8% [53].

In an alternative approach, Khan et al. [54] developed a label free aptasensing platform based on the specific interaction of a NH_2-modified aptamer with carboxy-amine polyethylene glycol chain (PEG) previously chemically grafted on screen-printed carbon electrodes (SPCEs). The carboxy-amine PEG proved to be an effective spacer for the formation of a tunnel for the electron transfer from the redox probe to the electrode surface. The conformational changes of the aptamer induced by analyte binding, resulted in the increase of the resistance to the charge transfer, which was measured using electrochemical impedance spectroscopy with a limit of detection of 2.8 ng/L. Analyses of spiked samples showed a toxin recovery of up to 99% [54].

Whilst fluorescence resonance energy transfer (FRET)-based aptasensors have been reported to have excellent sensitivity [55,56], the combination of the fluorescent dye FAM with magnetic reduced GO also exhibits excellent sensitivity and has been applied to the detection of patulin. As can be seen in Fig. 2, the fluorescence of the FAM-labeled PAT aptamer is quenched in the presence of the rGO-Fe_3O_4. Upon interaction of the PAT aptamer with its cognate target, it is displaced from the rGO-Fe_3O_4, and then isolated through magnet separation. Addition of DNase I cleaves the free aptamer complex, releasing them for additional cycles of target recognition and this approach of signal enhancement resulted in a 13-fold lowering of the detection limit to 0.28 ng/L [56].

A simple ratiometric fluorescent sensing platform was proposed by Ahmadi et al. [57] for detection of patulin using target-induced strand displacement composed of two fluorescent dyes, Carboxyfluorescein (FAM) and Carboxytetramethylrhodamine (TAMRA) (see Fig. 3). A DNA duplex is formed between the aptamer flanked with an oligonucleotide tail and a sequence partially complementary to the tail labeled with FAM (cDNA1) as well as with a sequence partially complementary to the aptamer that is labeled with TAMRA (cDNA2), bringing the two fluorophores in proximity, resulting in FRET. Upon the addition of the patulin, the TAMRA labeled sequence is displaced moving the TAMRA too far away from the FAM for FRET to occur, thus leading to a reduction in fluorescence emission. The limit of detection for this assay was 6 ng/L [57].

2.2. T-2

T-2 mycotoxin is one of the most toxic trichothecene mycotoxins produced by various species of *Fusarium*, including *Fusarium acuinatum, Fusarium poae, Fusarium langsethiae,* and *Fusarium sporotrichioide* [58–60]. The toxin is widely distributed in oats, maize, grains, barley, rice, and wheat, as well as in some cereal-based products and is found all over the world [61]. T-2 is a serious risk to humans and animals, leading

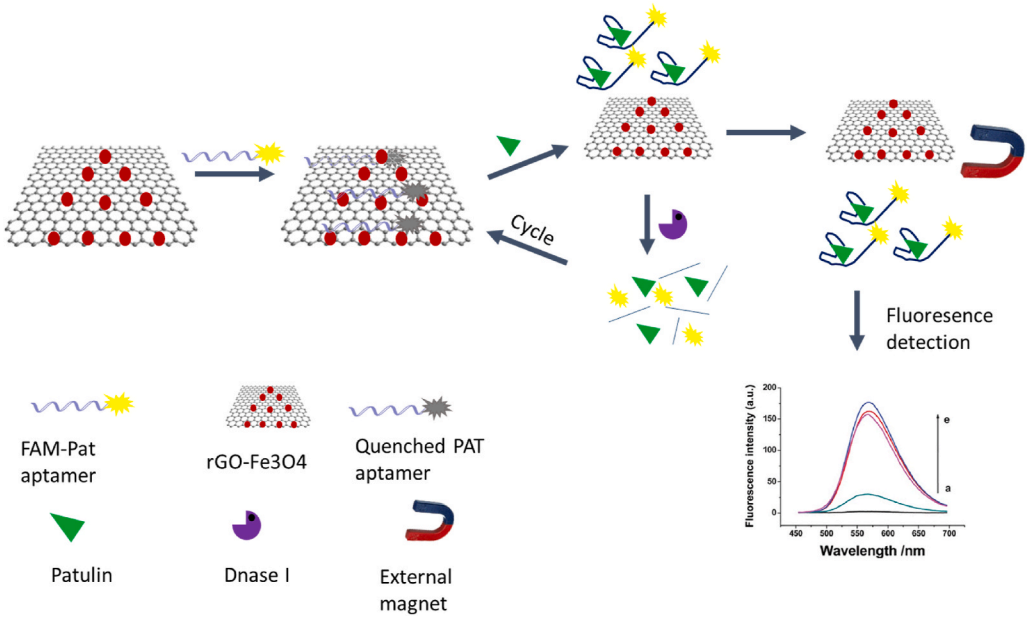

Fig. 2. Aptamer-based fluorescent detection of patulin.

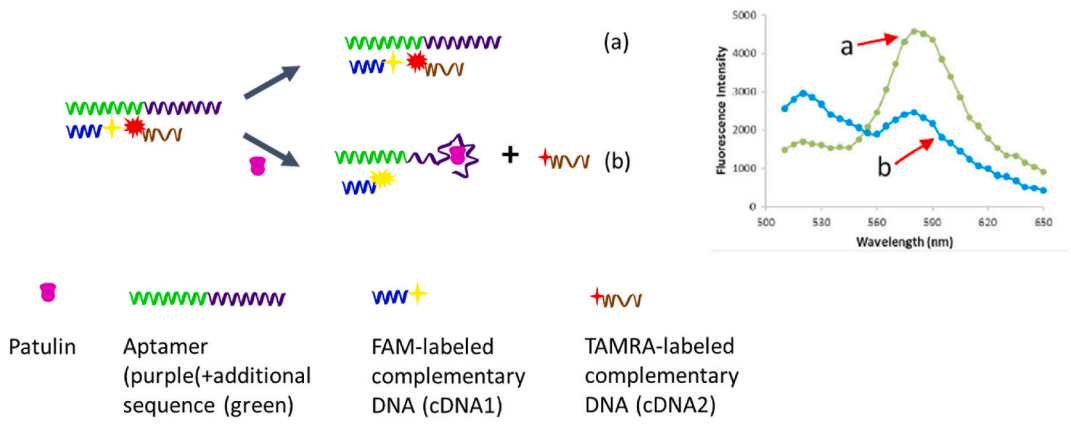

Fig. 3. Schematic diagram of the function of ratiometric fluorescent aptasensor for detection of patulin.

to emesis, diarrhea, lethargy, weight loss, hemorrhage, immune suppression, necrosis, cartilage damage, apoptosis, and even death [62]. T-2 toxin is type A trichothecene and their main mode of action is through inhibition of protein synthesis by binding to ribosomal RNA that disrupts cell membranes [63–65]. The T-2 toxin is thus considered to be one of the most dangerous contaminants by the European Food Safety Authority (EFSA) [65].

Currently, instrumental analysis for T-2 detection includes ultra-performance liquid chromatography−tandem mass spectrometry (UPLC−MS/MS)[66], gas chromatography−tandem mass spectrometry (GC−MS/MS) [67], liquid chromatography−tandem mass spectrometry (LC−MS/MS) [65] and ELISA [68].

Recently, Chen et al. [69] generated a high-affinity ssDNA (single--strand DNA) aptamer that specifically binds to the T-2 toxin. After 10 rounds of GO-SELEX the preferred aptamer demonstrated a low dissociation constant (K_d) of 20.8 ± 3.1 nM and excellent selectivity towards T-2 toxin. Using the selected aptamer as the recognition element, a fluorescent bioassay was developed for the measurement of T-2 in beer samples with a linear range from 0.5 to 37.5 μM and a limit of detection of 0.4 μM [69].

In the work published by Zhong et al. [70] glassy carbon electrode (GCE) were modified with molybdenum disulfide-polyaniline-chitosan-gold nanoparticles (MoS_2-PANI-Chi-Au) followed by immobilization of an amino-terminated capture DNA probe by Au–N bonds. A mixture of T-2 toxin and its aptamer was pre-incubated for 120 min and then added to the surface of the modified electrode. Any free T-2 toxin aptamer that has not formed a complex with T-2 in the sample partially hybridizes with the surface-tethered capture probe and subsequently reduced graphene oxide-tetraethylene pentamine-gold@platinum nanorods (rGO-TEPA-Au@Pt NRs)-signal DNA probe is added and partially hybridizes with the T-2 toxin aptamer, resulting in a signal amplified through the catalysis of hydrogen peroxide and measured using chronoamperometry. The presence of the T-2 toxin in the sample under interrogation will bind to the aptamer, preventing formation of this complex and thus the signal observed is inversely proportional to the concentration of the T-2 [70].

In another work, aptamer functionalized silver nanoclusters (apt-AgNCs) were used as fluorescent dyes, while MoS_2 (molybdenum disulfide) was used as fluorescent quenchers (see Fig. 4). The apt-AgNCs adsorb on the surface of MoS_2 nanosheet via van der Waal forces, resulting in quenching of the fluorescence intensity. When T-2 toxin is present, the interaction between AgNCs and MoS_2 is weakened and the fluorescent signal gradually recovered and is proportional to the T-2 toxin concentration. Addition of a poly-thymine (T5) linker sequence to

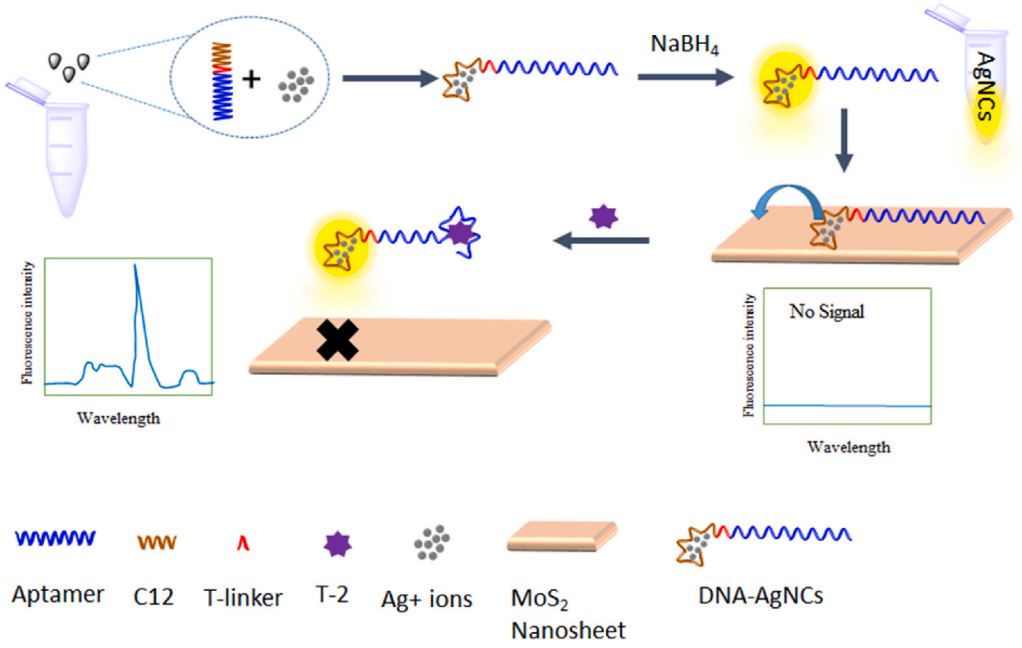

Fig. 4. Illustration of sensing module for T-2 toxin detection based on fluorescence quenching from DNA-AgNCs to MoS_2 nanosheet.

the aptamer resulted in a higher fluorescence signal [71].

2.3. Aflatoxin B1

Aflatoxin B1 (AFB1) is a highly toxic mycotoxin produced by *Aspergillus flavus*, *A. parasiticus*, and *A. nomiu* [72]. It is highly oncogenic, teratogenic and mutagenic, and is classified as group 1 A carcinogen by the International Agency for Research on Cancer (IARC) [73]. Prevalent mycotoxins can readily pollute food and feedstuffs at different stages, including pre-harvest, post-harvest, storage, transportation and consumption [74–76]. Consequently, methods for sensitive and rapid detection of AFB1 are urgently required. Currently, many analytical methods, including chromatography and immunological methods [77, 78] have been used for the detection of AFB1. Again, these laboratory-based methods are time consuming, not simple to perform, require multiple steps and expensive instrumentation.

Due to its importance, several aptamers have been selected against AFB1. Ma et al. [79] selected a highly specific aptamer with a K_d of 11.39 nM, whilst, Setlem et al. [80] identified 2 different sequences with K_d values of 50.45 ± 11.06 and 85.02 ± 25.74 nM, respectively. These aptamers were used in ELONA (Enzyme-linked oligonucleotide assay) and HPLC analysis, achieving detection limits of 20 and 40 ng/mL. Spiking studies and HPLC analysis in corn samples showed a good limit of quantification. Finally, the Neoventures Biotechnology Company (Canada, https://neoventures.ca/) developed an aptamer which has been used in several assays and sensors. Geleta et al. [81] developed an electrochemical aptasensor combining the aptamer selected by Neoventures with reduced graphene oxide/molybdenum disulfide/polyaniline@gold nanoparticles (RGO/MoS_2/PANI@AuNPs/Apt) achieving good reproducibility and an impressively low LOD of 0.002 fg/mL. In another study, an alternative electrochemical sensing strategy was reported by Peng et al. [82]. AFB1 aptamer-incorporated tetrahedral DNA nanostructures (TDNs) were combined with 3DOM MoS_2–AuNPs film for the construction of the sensing interface. Following interaction with AFB1, aptamers were released from the electrode surface and hybridization-free TDNs were formed. Bio composites of DNA helper strands (H1) and HRP (Horseradish Peroxidase Assay) functionalized AuNPsSiO_2@Fe_3O_4 nanospheres hybridise with the hybridization-free TDNs. The current response coming from the HRP-catalyzed reduction of H_2O_2 using thionine as an electrochemical probe was proportional with the AFB1 concentration, again with an impressive detection limit of 0.01 fg/mL.

An alternative electrochemical approach was developed by Abnous et al. [83], and was based on an aptamer complex that forms a π-shape structure of the aptamer complexed with its complementary DNA, where the π-shape structure disassembles in the presence of AFB1, and following addition of Exonuclease 1, a high current was measured, achieving a much higher detection limit of 2000 fg/mL.

Using a combination of Exo III, aptamer and telomerase Zheng et al. [84] designed an extremely sensitive aptasensor, achieving a detection limit of 0.6×10^{-4} ppt. Wang et al. [85] developed an impedimetric, label free aptasensor based on screen printed carbon electrodes modified with Fe_3O_4@Au/aptamer nanoparticles. The developed method had a linear range of 20–50 ng/mL with a detection limit of 15 pg/mL and was successfully applied to the detection of AFB1 in spiked samples of peanuts.

Surface Plasmon Resonance (SPR) is a label-free optical detection platform, that measures kinetics and affinity of bimolecular interactions in real-time and is frequently applied to the determination of dissociation constants for larger molecules but can be challenging to adapt to small molecules [86]. SERS (Surface-enhanced Raman spectroscopy) is a nondestructive molecular spectroscopy method [87], and powerful fingerprint analytical technique, that has been widely applied for trace detection in food safety [88], biomedicine [89,90], and environmental monitoring [91]. The high sensitivity of SERS is mainly attributed to the local electromagnetic enhancement (EM) caused by surface plasmon resonance (SPR) of coinage metal nanomaterial (such as Au, Ag and Cu) [92,93]. This technique for AFB1 detection was proposed by different groups.

Highly selective and sensitive detection of AFB1 was reported by Li et al. [28]. The aptamer for AFB1 was partially hybridized with complementary DNA, which was released upon interaction with AFB1 and immediately hybridized with hairpin DNA on the surface of a sputtered Au film. Exonuclease III hydrolyzed the double-stranded DNA, leaving short single-stranded DNA on the Au surface and releasing complementary DNA for the next ring opening and digestion. A SERS tag was captured on Au surface via DNA hybridization. This sensor achieved a limit of detection of 0.4 fg/mL, and was also used for the quantification of AFB1 levels in spiked peanut samples, achieving recoveries in the range of 89–121%.

Wu et al. [94] developed a SPR system where streptavidin was immobilized on the surface of CM5 and linked to biotinylated aptamer. As expected, the aptasensor showed high specificity towards AFB1 and AFB2, but not to the other mycotoxins. The LOD was 0.19 ng/mL, and AFB1 was detected in vinegar, achieving recoveries in the range 96.3–117.8%. Sun et al. [95] used the same assay for red wine and beer real samples with a biosensor with a linear range from 0.4 nM to 200 nM with a 0.4 nM detection limit. Zhao et al. [96] developed SERS for the double detection of 2 different mycotoxins, AFB1 and OTA in real samples. The limits of detection were 0.006 ng/mL for OTA and 0.03 ng/mL for AFB1.

In a study reported by Yang et al. [97], amino-terminated aptamer conjugated magnetic-bead (CS–Fe_3O_4) and gold nanotriangles (GNTs)-DTNB@Ag-DTNB nanotriangles (GDADNTs), were used as the capture and the reporter of AFB1, respectively. The Raman reporters were loaded in the gap of the GNTs@Ag and on the surface of GNTs-DTNB@Ag, respectively and then modified with aptamer to assemble GNTs-DTNB@Ag-DTNB-aptamer for reporter nanoprobe, which performed better SERS intensity.

A colorimetric assay measures a color change of a reagent in the presence of an analyte [98]. Jafari et al. [99] designed an aptasensor using the combination between AFB1 specific aptamer and a horseradish peroxidase-mimicking DNAzyme. DNAzymes and aptamers have reported advantages over protein enzymes [100–102] and the same research group demonstrated the catalytic activity and efficiency of aptamer–DNAzyme using both circular dichroism (CD) spectroscopy and biochemical analysis [103]. Seok et al. [104] designed a colorimetric assay where split halves of hemin-binding DNAzymes were combined with an AFB1 aptamer to generate a homogeneous colorimetric sensor that undergoes an AFB1 induced structural deformation of the aptamer-DNAzyme complex, resulting in a split of the DNAzyme halves and a concomitant reduction in peroxidase mimicking activity, achieving a detection limit of 0.1 ng/mL. Shim et al. [105] developed a chemiluminescence competitive aptamer assay for AFB1 using a hemin/G-quadruplex horseradish peroxidase-mimicking DNAzyme (HRP-DNAzyme) linked with an AFB1 aptamer. Under optimized conditions the assay gave a limit of detection of 0.11 ng/mL.

Sun et al. reported a competitive enzyme linked oligonucleotide assay, where the wells of a microtiter plate was coated with a BSA-AFB1 complex that competed with AFB1 in the sample for binding to a HRP-labeled aptamer, with an inverse relationship between signal and concentration, achieving a limit of detection of 0.01 nM [106].

Joo et al. also exploited the fluorescence quenching property of GO in an assay using FAM-labeled AFB1 aptamer, which was pre-incubated with the sample. Following the addition of GO, any aptamer not bound to AFB1 adsorbs on to the GO, resulting in a decrease in the fluorescence intensity of the system. When the assay was applied to a real sample, the limit of detection was 4.5 ppb [107]. Zhang et al. also used GO but in a different approach, exploiting the ability of GO to protect aptamers from nuclease cleavage [108], whilst Wang et al. developed fluorescent nitrogen-doped carbon dots (N, C-dots), which were synthesized by the hydrothermal treatment of pancreatin and assembled on aptamer/-AuNPs via electrostatic interactions [109]. Addition of AFB1 displaced the aptamer N, C-dots with a concomitant change in fluorescence intensity, achieving a detection limit of 5 pg/mL. Lu et al. designed a system where the fluorescence of the thiolated aptamer chemisorbed on Q-dots is strongly quenched by GO. Upon addition of AFB1, fluorescence is restored and the assay had a detection limit of 1.0 nM [110].

In an alternative format, Chen et al. performed a fluorescent assay via the formation of a duplex between a fluorescein labeled AFB1 aptamer and a partially complementary oligonucleotide tethered with a quencher moiety. Upon binding to AFB1, the latter was displaced, resulting in restoration of the fluorescence signal, which was proportional to the concentration of DNA, with an LOD of 1.6 ng/mL. This method was successfully applied for the analysis of AFB1 in infant rice cereal with satisfactory recovery in the range of 93.0–106.8% [111].

Sabet et al. apply a FRET-based method, in which aptamer-conjugated Quantum dots (QDs) are adsorbed to Au nanoparticles (AuNPs), thus quenching the fluorescence of the QDs, which is restored upon addition of AFB1 due to displacement of the aptamers from the AuNPs, achieving an LOD of 3.4 nM [112]. In a similar type of approach, Goud et al. developed a simple TAMRA (tetramethyl-6-carboxyrhodamine) quenching-based aptasensing platform, where they exploited the interaction of FAM-labeled aptamer with complementary TAMRA-labeled DNA, where again AFB1-induced displacement restored fluorescence, and the method exhibited good sensitivity, good selectivity with a limit of detection of 0.2 ng/mL [113].

In another approach, Liu et al. described magnetic solid-phase extraction (MSPE), where AFB-biotinylated aptamers were immobilized on streptavidin coated magnetic agarose microspheres (MAMs), achieving LODs of 25 and 10 pg/mL for AFB1 and AFB2, respectively [114].

Recently, lateral flow assay (LFA) chromatographic strips using aptamer-functionalized nanogold particles for the detection of molecules have been established as promising tools. LFA is a simple paper-based platform for the detection of analytes, where the sample is placed on a test device and the results are displayed within 5–30 min. LFAs are typically composed of a nitrocellulose membrane, sample pad, conjugate pad, wicking or absorbent pad and backing pad [115]. Shan et al. developed a lateral flow assay using aptamer-functionalized nanogold particles for the detection of aflatoxin B1 (AFB1) and chloramphenicol (CAP), in a competitive assay format, where a biotinylated probe immobilized on a streptavidin coated test line competes with the analytes for binding to the aptamer, achieving a detection limit of 1.05 ppb [116].

Zhu et al., who developed a LFA with a dual competition for binding to a Cy5 labeled aptamer, one based on competition between target in sample and immobilized antigen, and the other based on competition between target in sample and immobilized complementary strand, achieving a detection limit of 0.1 ng/mL, with the LFA showing a good correlation with a commercial ELISA (Enzyme-linked immunosorbent assay) kit (Fig. 5). Their assay showed high sensitivity, specificity and reproducibility in all real samples that they analyzed [29].

A dipstick assay was developed by Shim et al., where they immobilized streptavidin and anti-cy5 antibody at the test and control lines, achieving a limit of detection of 0.1 ng/mL, and the dipstick was successfully applied to the analysis of corn samples [117].

Finally, Guo et al. developed another type of aptasensor using RT-qPCR (Quantitative reverse transcription PCR). Here, an AFB1 aptamer was used as a molecular recognition probe, while its complementary DNA played a role as a signal generator for amplification by real-time quantitative polymerase chain reaction (PCR). The assay was highly sensitive and specific, and relatively low cost but could not be deployed for in-field analysis as it requires pretreatment and the instrumentation is not portable [25].

Many more aptasensors have been developed for the detection of AFB1, due to its importance, and the performance characteristics of these are detailed in Table 1.

2.4. Aflatoxin B2

Aflatoxins B2 (AFB2) are highly toxic, teratogenic, mutagenic and carcinogenic metabolites produced by fungi of the genus *Aspergillus*, mainly *Aspergillus flavus, Aspergillus parasiticus* and *Aspergillus nomius* [118–120]. These toxins are present in grain, nuts, cottonseeds, and other commodities associated with agricultural products or animal feed [121]. Studies have revealed that aflatoxin species show immunosuppressive effects as a result of the inhibition of DNA, RNA and protein synthesis through different mechanisms [122,123]. For example, aflatoxin may cause rapid death, while hepatocellular carcinoma develops as a chronic outcome when exposed to a high dose of aflatoxin. Concerning consumer health, maximal residue limits for AFs in foods and

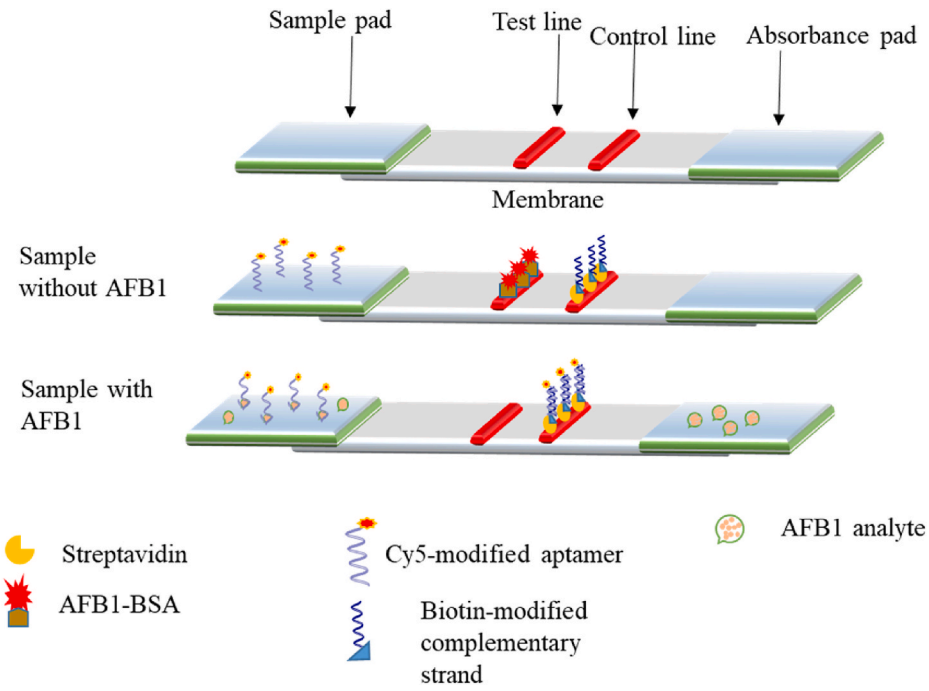

Fig. 5. Configuration of a dual-competitive lateral flow assay for detection of AFB1 where in the absence of AFB1, a Cy5-modified aptamer is captured by an AFB1-BSA conjugate immobilized on the test line, whilst in the presence of target in the sample the Cy5-aptamer binds to it rather than to the surface immobilized AFB1.

raw stuff have been established by the governments of many countries. The International Codex Alimentarius Commission and the EU have adopted the maximum residues limits (MRL) of aflatoxins (B1 + B2 + G1 + G2) for 15 ng/mL in different foods [124,125].

As is the case for AFB1, different methods have been established for the separation and qualitative/quantitative detection of AFB2, such as thin-layer chromatography [126], high-performance liquid chromatography [127–130], and enzyme-linked immunosorbent assay [131], but these are inherently laboratory based techniques [132].

A highly specific AFB2 aptamer, with a K_d of 9.83 nM was successfully selected by Ma et al. and was used to construct a fluorescent biosensor that had a wide linear range from 100 to 1800 ng/L and a detection limit of 50 ng/L. Additionally, the spiked recovery experiment of AFB2 in peanut oil sample exhibited a recovery ratio between 94.0% and 101.6% which showed good accuracy of the proposed aptamer-based bioassay [79].

In another study, Luan et al. [133] developed a simple sensor for colorimetric detection of AFB2 using gold nanoparticles. In the absence of AFB2, the aptamers coat the gold nanoparticles and protect it from aggregation, whilst in the presence of AFB2 the aptamers are not free for coating the nanoparticles, which then aggregate (Fig. 6), with the degree of aggregation proportional to the concentration of the AFB2 present in the sample. The use of nanoparticles is analytically attractive because the red-to-blue AuNP color change in the presence of AFB2 is easily measured by a spectrophotometer or even observed by the bare eyes. The method demonstrated a linear dynamic range of 0.025–10 ng/mL of AFB2 with a detection limit of 0.025 ng/mL, which is lower than the MRL (Maximum Residue Level) in edible food as set by China and the European Commission. Moreover, in the presence of AFB1 as interference, the method was able to detect AFB2 with high selectivity. This AFB2 detection method provides several advantages over other analytical techniques with high sensitivity, high stability, quick analysis time, and cost effectiveness in food and agricultural products [133].

2.5. Zearalenone

Zearalenone (ZEN; also known as F-2 toxin), is produced by several *Fusarium* species [134,135] with widespread occurrence in the crops like corn, maize, barley, oats, rice and sorghum. There is evidence that the consumption of ZEN contaminated products causes severe adverse effects, such as neurotoxicity, carcinogenicity, and immunotoxicity [134,136]. Furthermore ZEN can impair reproduction [137,138]. Therefore, innovation in the design of analytical techniques for the detection of ZEN is also vitally important. Similar to the other mycotoxins, various methods have been employed for the determination of ZEN contents in foods or feedstuffs, including (i) instrumental analysis, such as high-performance liquid chromatography with either fluorescence detector or mass spectrometric detection and (ii) immunoassays including enzyme-linked immunosorbent assay (ELISA) and lateral flow assays [139–143]. Instrumental analytical methods provide good performance in terms of accuracy, precision, sensitivity, and reproducibility, but as previously stated, they are inappropriate for onsite rapid analysis because they require tedious sample preparation, expensive equipment, and highly skilled operators. Immunochromatographic assays can be used for rapid qualitative screening [144,145], but they often fail to provide accurate quantitative results and a definite confirmation of the mycotoxin ZEN because the antibodies in immunoassays are sensitive to temperature and require strict physiological conditions for use. In addition, the production of antibodies requires animals or cell cultures in a time consuming and costly production. Therefore, it is crucial to develop some new recognition molecules for ZEN, such as aptamers, that are easier to produce and more stable.

Chen et al. [146] described the isolation and identification of an aptamer recognizing ZEN using magnetic bead SELEX resulting in a high affinity aptamer with a K_d of 41 ± 5 nM, and successfully applied this aptamer to the specific detection of ZEN in real samples exploiting a pre-concentration using biotinylated aptamer on streptavidin-coated magnetic beads. The bead suspension was analyzed through confocal imaging to observe the binding between aptamer and ZEN using an LSM 700 laser scan confocal microscope and analyses with β-ZOL (β-zearalenols), AFB1, AFB2, FB1, and FB, showed excellent specificity of the selected aptamer. This pre-concentration was used to determine ZEN in beer samples, and in comparison with ELISA, an excellent degree of correlation was obtained ($p < 0.0001$), with acceptable recovery rates

Table 1
A summary of the mycotoxin apatasensors and their parameters.

Toxin	Assay	Materials	Recovery rate	LOD	Linear range	Selectivity	Real sample	Ref.
PAT	FAM-AptPAT-rGO-Fe_3O_4	rGO-Fe_3O_4	77–104%	0.28 μg/L	0.5–30 μg/L	AFB1,DON,T-2,TA	apple juice and grape juice	[56]
PAT	Fluorescence	FAM/TAMRA	94–109	6 ng/L	15 ng/L-35 μg/L	AFB1,DON,AFM1,ZEN	apple juice	[57]
PAT	Voltammetric	MCH/DpAu/ZnO NR chitosan on a gold electrode	95.6–104.8%	0.27 pg/mL	5*10-8-5*10–13 g/mL	AFB1,DON,FB1,ZEN	apple juice	[53]
PAT	Impedimetric	Peg/SPCE/NH2aptamer	99%	2.8 ng/L	1–25 ng/L	OTA,ZEN,AFB1	apple juice	[54]
PAT	Electrochemical	aptamer-AuNP-BP NSs/GCE	97.3–104.6%	0.03 nM	0.1 nM-10 μM	OTA,ZEN,AFB1	apple juice	[189]
PAT	Colorimetric	enzyme-chromogenic	93–108.8%	48 pg/mL	50–2500 pg/mL	N.A.	apple juice	[51]
ZEN	Electrochemical	CP1–Au-Thi and CP2–Au/ $rMoS_2$-Au	95.9–105.2%	$5*10^{-4}$ ng/mL	$1*10^{-3}$-10 ng/mL	T-2,FB2,OTA,AFB1	maize	[166]
ZEN	Electrochemical		93.8–102.4%		$1*10^{-3}$-$1*10^{2}$ ng/mL		maize	
ZEN	ELONA/ELISA	antibody/aptamer	95–105%	0.01 ng/mL	0.03–2.5 ng/mL	AFB1, AFB2, DON	corn	[190]
ZEN	Magnetic separation	Magnetic beads	85.0–105.1%	0.25 ng/mL	3.14×10^{-9}–3.14×10^{-5} M	β-ZOL, AFB1, AFB2, FB1, and FB2	beer	[146]
ZEN	Colorimetric aptasensor	AuNPs/exonuclease III	95–103%	10 ng/L	20–80 000 ng/L,	OTA, AFM1, AFB1, DON	spiked human serum	[152]
ZEN	Lateral flow test strip	nanoparticles/aptamer	93.4–114.2%	20 ng/mL	5–200 ng/mL	DON,OTA, FB1, AFB1	corn	[168]
ZEN	Fluorescence	MNPs/TRFL	Wheat:90.04–114.75% Maize: 80.76–119.66%	0.21 pg/mL	0.001–10 ng/mL	OTA, AFB2, DON and Patulin	wheat and maize	[164]
ZEN	Electrochemical	Cu@L-Glu/Pd–PtNP	92–105%	0.45 fg/mL	1 fg/mL-100 ng/mL	T-2, OTA, AFB1, FB1	N.A.	[167]
ZEN	Fluorescence	UCNPs/MNPs	Corn: 94.26–104.30% Beer: 93.39–105.53%	0.007 μg/L (corn) 0.126 μg/L (beer)	0.05–100 μg/L	AFB1, AFB2, OTA, FB1 and FB2	corn and beer	[153]
ZEN	Colorimetric	gold nanoparticles	92–110%	10 ng/mL	10–250 ng/mL	OTA, AFB1	corn/corn oil	[51]
ZEN, T-2, AFB1	Fluorescence	tungsten disulfide(WS_2)	ZEN: 94.4–98% T-2: 90–92% AFB1: 87–96%	ZEN-0.51 T-2-0.33/ AFB1 0.40 pg/mL	0.001–100 ng/mL	N.A.	maize	[165]
ZEN	Colorimetric	Au NPs	94.42–99.78%	4 ng/mL	4–128 ng/mL	a-ZON, β-ZON, AFB1, T-2, and FB1	corn powder	[191]
ZEN	Electrochemical/ luminescence	NGQDs–NH_2–Ru@SiO_2 luminophore	92.2–111.1%	1 fg/mL	10 fg/mL-10 ng/mL	OTA, AFB1, FB1	corn flour	[192]
ZEN	Fluorescence	Functional GO	Beer: 87–95.3% Wine: 93–95.8%	1 ng/mL	4–16 ng/L	OTA,OTB,AFB1/M1,PAT	beer, wine	[160]
ZEN	Electrochemical	CS@AB-MWCNTs/CGO-ZBA	101.2–111.5%	3.64 fg/mL	10 fg/mL- 1 ng/mL	AFT,OTA, β-ZAL	corn oil/corn flour	[193]
ZEN	Fluorescence	FAM aptamer/MSNs-NH_2	83.3–101.5%	0.012 ng/mL	0.005–150 ng/mL	OTA,FB1,T-2,DON	cereals, maize, rice, beer	[194]
ZEN, FB1, OTA	SERS/Fluorimetry	FRET/aptamer	90–107%	ZEN-0.03 ng/mL FB1-0.02 pg/mL OTA-0.01 ng/mL	ZEN-0.1–100 ng/mL FB1-0.05–200 pg/mL OTA-0.05–25 ng/mL	OTA,FB1, T-2, ZEN, PAT, AFB1	corn	[195]
T-2	Fluorescence	NC-T5-apt-AgNCs/MoS_2 nanosheet	Maize: 89.46–102.08% Wheat: 90.41–107.75%	0.93 pg/mL	0.005–500 ng/mL	DON,FB1,AFB1,OTC,ZEN,OTB	maize, wheat	[71]
T-2	Electrochemical	GCE/MoS_2-PANI-Chi-Au/(rGO-TEPA-Au@Pt NRs	94.6–103.52%	1.79 fg/mL	10 fg/mL-100 ng/mL	ZEN,OTA,FB1,AFB1	canned beer	[70]
T-2	FAM-labeled	FAM-labeled	93.6–106%	0.4 μM	0.5–37.5 μM	FB1, ZEN, AFB1, OTA,	beer	[69]
FB1	Electrochemical impedance spectroscopy (EIS)	AUNPs/glassy carbon electrode	91–105%	2 pM	0.1 nM to 100 μM	FB-1, AFB-1, ZEN, and T-2	maize	[27]
FB1	HPLC		N.A.	N.A.	N.A.			[171]
FB1	Fluorescence	rGO/Ni/PtNPs	FB1: 104%, OTA: 108%, White Wine: 105%	FB1: 0.0007 μg/mL, OTA: 0.004 μg/mL	FB1: 0.005–1 μg/mL, OTA; 0.01–10 μg/mL	N.A.	beer, white/red wine	[196]
FB1	Fluorescence	rGO/PtNPs	Beer: FB1-90-106%, Wine OTA -90-102%	0.2 μg/mL for FB1, 0.002–0.01 μg/mL for OTA	FB1: 0.001–10 μg/mL, OTA: 0.01–10 μg/mL	N.A.	wine and beer	[197]

(*continued on next page*)

Table 1 (*continued*)

Toxin	Assay	Materials	Recovery rate	LOD	Linear range	Selectivity	Real sample	Ref.
FB1	Fluorescence	SPCM/aptamer	OTA: 81.8–116.38%, FB1: 76.58–114.79%	0.25 pg/mL for OTA and 0.16 pg/mL for FB1	0.01–1 ng/mL for OTA, and 0.001–1 ng/mL for FB1	AFB1, OTA, and FB2	rice, corn, and wheat	[178]
FB1	Fluorescence	CdTe QDs/(GO)/Fe_3O_4/GQDs and RQDs	AFB1: 95–97%, FB1: 92–96%	AFB1: 6.7 pg/mL, FB1: 16.2 pg/mL	AFB1: 10 pg/mL-100 ng/mL, FB1: 50 pg/mL-300 ng/mL	OTA,OTB,AFB2,AFM1	N.A.	[176]
FB1	SERS/Fluorescence	SERS/AuNR/Cy5 aptamer	92–107%	SERS: 3 pg/mL, Fluorescence: 5 pg/mL	10–250 pg/mL	AFB1,ZEN,PAT,OTA,FB2,FB3	corn	[175]
FB1/ OTA	Time-resolved fluorescence NPs	($NaYF_4$:Ce, Tb and NH_2-Eu/ DPA@SiO_2	FB1: 89–110%, OTA: 90–109.66%	FB1-0.019 ng/mL OTA-0.015 ng/mL	0.0001–0.5 ng/mL	FB1/OTA	maize	[198]
OTA/ FB1	Multiplexed Fluorescence Resonance	UCNPs/GO/$BaY_{0.78}F_5$:$Yb_{0.}$, $Er_{0.02}$/ $BaY_{0.78}F_5$:$Yb_{0.}$, $Tm_{0.02}$	OTA: 94.13–119.30%, FB1: 84.32–124%	OTA: 0.02 ng/mL, FB1 : 0.1 ng/mL	OTA: 0.05–100 ng/mL, FB1: 0.1–500 ng/mL	AFB1/B2/G1, FB2,ZEN	maize	[173]
OTA/ AFB1	Fluorescence	Fe_3O_4@Au/SiO_2@gQDs	95–108%	OTA- 0.67 pg/mL AFB1- 1.70 pg/mL	OTA-0.002–5 ng/mL AFB1-0.005–10 ng/mL	FB1, AFB2,OTB	corn	[199]
OTA/ AFB1	Fluorescence	DNA/AgNCs/Zn II	OTA: 88.1–113.5%, AFB1: 88.1–116.8%	OTA: 0.3 pg/mL, AFB1: 0.2 pg/mL	0.001–0.05 ng/mL	OTB,DON,ZEA	wheat	[200]
AFB1	Fluorescence	AFB1 aptamer/thioflavin T-and AFB1 aptamer/AFB	74.7–121%	0.2 ng/mL	0.2–200 ng/mL	AFB2.AFG1/G2/M1,FB1/B2, OTA/B,NEO,PAT,ZEN,CTA,HT-2,CTIV,CIT	peanut, beans, cereal, alcoholic beverage, and fermented condiment	[201]
AFB1	Fluorescence	TAMRA/FAM	Beer: 93–102%, Wine: 89–103%	0.2 ng/mL	0.25–32 ng/mL	AFM1	beer, wine	[113]
AFB1	Fluorescence	CdZnTe QDs/SiO_2/AuNPs	95.7–106.3%	0.2 ng/mL	0.05–100 ng/mL	AFB2, OTA, FB1	peanut	[202]
AFB1	Fluorescence	FAM/GO	97–107%	4.5 ppb	4.5–300 ppb	AFB2, AFG1, AFG2	rice seeds	[107]
AFB1	Fluorescence	Fe_3O_4@oMWCNTs/split G-quadruplex/hemin DNAzyme	98.20–101.60%	0.02 ng/mL	0.5–0.15 ng/mL	AFB2, AFM1,AFG2, glucose, fructose,maltoze	peanut, maize, wheat, pearl rice, aromatic rice and red rice	[203]
AFB1	Fluorescence	SNPs/N-methyl mesoporphyrin IX/crimera	95–106%	8 pg/mL	30–900 pg/mL	OTA,MC-LR,AFB1,DON	serum and grape juice samples	[204]
AFB1	Fluorescence	N,C-dots/Aptamer/AuNPs	92–105%	5 pg/mL	5pg/mL-2 ng/mL	OTA,FB1,DON,ZEN,AFB2,AFG1	peanut, corn	[109]
AFB1	SERS	Au film/aptamer/Exo III	89–112%	0.4 fg/mL	$1*10^{-6}$-1 ng/mL	DON,ZON,AFG1/G2/M1/B2	peanut	[28]
AFB1	SERS	AuNR@DNTB@Ag nanorods/ DNTB	91.09–105.73%	0.0036 ng/mL	0.01–100 ng/mL	OTA,FM1	peanut oil	[205]
AFB1	FRET	QDs/AuNPs	103.0–108.0%	3.4 nM.	10–400 nM	AB2,AM2, AG2	rice and peanut	[112]
AFB1	Fluorescence	Fluorescence label aptamer	93.0–106.8%,	1.6 ng/mL	5–100 ng/mL	AFB1,OTA, AFB2,AFG1, AFG2, AFM1, ZEA, FB1	infant rice cereal	[111]
AFB1	Fluorescence	ROX labeled aptamer/GO/ nuclease	82.4–117%	10 ng/mL	12.5–312.5 ng/mL	AM1	corn sample	[108]
AFB1	Electrochemical	AuNPs/Exo III	95–110%	$0.6*10^{-4}$ ppt	0.1–100 ppt	OTA, OTB, DON	corn	[84]
AFB1	SERS	Ag@Au CS/NPs	95.00–99.65%	0.03 ng/mL	0.05–100 ng/mL	OTB,OTC, AFB2,AFG1, AFG2, FB1,L-Cys,BSA,GSH, warfarin	maize meal	[96]
AFB1	Colorimetric	DNAzyme-hemin/aptamer	93.96–104.95%.	0.1 ng/mL	0.1–1 ng/mL	AFG1,AFG2, ZEA,T-2,DON, CIT	corn	[104]
AFB1	RT-qPCR	Aptamer	88–127% wildrye hay 94–119% rice cereal	25 fg/mL	$5.0*10^5$-5.0 ng/mL	OTA,ZEN,FB1, AFM1,α-ZOL, AFB2, AFG1,AFG2	infant rice cereal	[25]
AFB1	Lateral flow	Cy5 aptamer	92.7–134.4%	0.1 ng/mL	0.1–1000 ng/mL	AFB1,AFB2,AFM1,AFM2,AFG1, AFG2,OTA,SM,ZEN	11 kinds of food and feedstuff samples	[29]
AFB1	Chemiluminescence	Aptamer/HRP-DNAzyme	60.4–105.5%	0.11 ng/mL.	0.1–10 ng/mL	AFB2,AFG1, AFG2,AFM1, OTA, ZEN,T-2 PAT	corn samples	[105]
AFB1	Dipstick assay		74–112%	0.1 ng/mL		AFB2,AFG1,AFG2,ochratoxinA, zearalenone, citrinin,T2 toxin, deoxynivalenol,andpatulin	corn	[117]
AFB1	SPR	Sensor chip/aptamer	87–102%	0.4 nM	0.4–200 nM	OTA,FB1, FB2,ZEN	red wine and beer	[95]
AFB1	Chemiluminescence	HRP/BSA-AFB1		0.01 nM	0.2–2 nM	OTA, FB1, FB2 and ZAE	white wine, maize flour	[106]

(*continued on next page*)

Table 1 (*continued*)

Toxin	Assay	Materials	Recovery rate	LOD	Linear range	Selectivity	Real sample	Ref.
AFB1	Immunoassay	Antibody/aptamer	73–98.80%	5 ng/mL		AFB1, AFB2, AFG1, AFG2, OTA, Citrinin, DON, FB1,	maize, paddy, corn, groundnut	[206]
AFB1	SELEX	AFB2, AFG1, AFG2, OTA,FB1	94.2–101.2%	35 ng/L	50–1.500 ng/L	AFB2, AFG1, AFG2, OTA,FB1	corn	[207]
AFB1	Fluorescence	Q-dots/GO		1.0 nM	3.2 nM - 320 μM	FB1, OTA, ZEN,DON	peanut oil	[110]
AFB1	Fluorescence	TPE-Z/GO	91.36–95.11%	0.25 ng/mL	0–3 ng/mL	FB1,OTA,BSA	corn, milk, rice	[208]
AFB1	Fluorescence	MSN-NH_2/Rh6G probe	89.70–94.70%	0.13 ng/mL	0.5–50 ng/mL	AFB1,AFB2,AFMI,DON,OTA, ZEN,T-2	corn oil, corn	[209]
AFM1	Fluorescence	GO	98–126%	0.05 μg/kg	0.2–10 μg/kg	AFB2,OTA,ZEN	infant milk powder	[210]
AFM1	Electrochemical	Fe_3O_4/PANi/IDE		1.98 ng/L	6–60 ng/L	OTA	milk	[211]
AFM1	Fluorescence	TAMRA/aptamer labeled	94.40–92.28%	5 ng/kg	25–2000 ng/kg	AFB1, OTA	milk	[212]
AFM1	EIS	Carbon SPEs	98–114%	1.15 ng/L	2–150 ng/L		milk	[213]
AFB1	Photoelectrochemical (PEC)	Ce–TiO_2@$MoSe_2$/Au	89.6–96.3%	0.01 ng/mL	0.03–200 ng/mL	AFM1,OTA,DON	no	[214]
AFB1	Fluorescence	thioflavin T	74.7–121%	0.2 ng/mL	0.2–1 ng/mL	AFG1,AFB2,FB1,FB2,OTA,OTB, PAT,ZEN,HT-2	peanut, beans (mung bean, and soya bean), cereal, beer and Chinese spirits, vinegar and soy sauce	[201]
AFB1	Ratiometric electrochemical	SiO_2 @PbS/CdTe QD-modifie Fe_3O_4@SiO_2	90–93.6%	4.5 pg/mL	5–50 mg/mL	FB1,OTA,AFB2	peanut	[215]
AFB1	Voltammetry	GCE/GO	94.58–104%	0.07 nM	0.5nM-4 μM	NO	human blood plasma, pasteurized cow milk	[216]
AFB1	Electrochemical	gold electrode		2 nM	8 nM-4 μM	OTA, OTB, FB1, FB2 and ZAE	beer and wine	[217]
AFB1	Chemiluminescence	SA-HRP	97.2–104.4%	0.2 ng/mL	0.5–40 ng/mL	AFG1,OTA,phytohormons found in peanut (t-ZR,IAA,GA3,JA)	peanut, milk	[218]
AFB1	Electrochemical	Fc cDNA/pβ-CD/AuNPs/GC	94.5–106.7%	0.049 pg/mL	0.1 pg/mL-10 ng/mL	AFB2, AFB2, FB1, DON, ZEA, SEB and OTA	peanut oil	[219]
AFB1	Electrochemical	GSPE/AF1-BSA/Bioaptamer	84–96%	0.086 ng/mL	0.1–10 ng/mL	AFG1	maize flour	[220]
AFB1	Optical sensor	AuNPs/t-DNA/PAPDI	96.3 −106.5%,	3.1 ng/mL	0.05–50 nM	OTA,AFB2,ZEN,FB1	maize	[221]
AFB1	Colorimetry	PGM-Based AFB1 Aptasensor Based on DNA Walker Machine	98.5 −103%	10pM	0.02–10 nM	AFB2, AFG1/2, DON, ZON AFM	bread	[222]
AFB1	Fluorescence	Fe_3O_4 @oMWCNT/split/aptamer	98.20-101.60%	0.02 ng/mL.	0.5-15 ng/mL	no	peanut, maize, wheat, pearl rice, aromatic rice and red rice	[203]
AFB1	Electrochemical	THI-rGO/Fc-Apt	86.5–112.0%	0.016 ng/mL	0.05–20 ng/mL	FB1, AFB2, ZEN, OTA	peanut	[223]
AFB1	Photoelectrochemical	reGO/P5FIn/Au	Wheat: 97.2 110.0%, Peanut: 98.3–106. %	0.002 ng/mL	0.01–100 ng/mL	N.A.	peanut, wheat	[224]
AFB1	Fluorescence	MPA-capped CdZnTe QDs/SiO_2 @QDs/AuNPs	95.7–106.3%	0.02 ng/mL	0.05–100 ng/mL	AFB2,FB1,OTA	peanut	[202]
AFB2	Colorimetric	AuNPs	89.4–92.9%	0.025 ng/mL	0.025–10 ng/mL	AFB1, AFG1 AFG2, OTA DDVP ETM	beer sample	[133]
OTA	Electrochemical impedance	AuNP/CuCoPBA	93.55-104.9%	5.2 fg/mL	50 fg/mL −10 ng/mL	BLM,AMP, RFP,ADR,AFB1	fruit juice	[225]
OTA	Fluorescence	DNA hydrogel/aptamer	92.1–105%	0.01 ng/mL	0.5–100 ng/mL	ZEN,T-2,AFB1	beer	[226]
OTA	Fluorescence	FRET/Cy5 aptamer	AFM1: 85.64–116.7%, OTA: 74.13–112.1%	AFM1-21 ng/mL OTA -330 ng/mL	AFM1/OTA-1 ng/mL-1 mg/mL	AFB1,ZEN,DON	milk, oat milk	[227]
OTA	Electrochemical	GCE/janus particles	95.7–100.18%	3.3×10^{-3} pM	1×10^{-5}-10 nM	OTB,ZEN,FB1	wine sample	[228]
OTA	Colorimetric	MnO_2 nanosheets/TMB	89.14–100.57%	0.069 nM	1.25–250 nM	OTB,AFB1,ZEA,ALT,Citrinin,TeA	grape juice	[229]
OTA	Electrochemical luminescence	CdS QDs/Cy 5-apt	Wine: 97.19–103.62%, Beer: 93.82–98.21%	0.012 nM	0.05–5 nM	AFB1,ZEN,FB1,DON,SEB	wine, beer	[230]
OTA	Electrochemical	SPGEs/Exo I	96.6–109.7%	0.7 pg/mL	0.001–100 ng/mL	OTB,AFB1,AFB2	beer	[231]
OTA	Electrochemical	AuNP/Fc/CP1	99.3–100.12	0.001 ppb	0.001–500 ppb	OTB,CAP,AFB1	wine	[232]
OTA		GCE/CdTe QDs/Cy5	96.1–100.7%	0.17 pg/mL	0.0005–50 ng/mL	FB1,DON,OTB	corn	[233]

(*continued on next page*)

Table 1 (*continued*)

Toxin	Assay	Materials	Recovery rate	LOD	Linear range	Selectivity	Real sample	Ref.
	Electrochemical luminescence							
OTA	Fluorescence	GO/Rnase H	90.9–112%	0.08 ng/mL	0.08–200 ng/mL	OTB,AFB1	wine	[234]
OTA	Fluorescence	CuNPs	standard deviation-5.02%	2.0 nM	2.5–250 nM	OTB,ZEA,AFB1,AOH,TeA, citrinin	red wine	[235]
OTA	Fluorescence	natural Fluorescence of OTA	89.8–100.7%	2 ng/mL		OTB, ZEN, citrinin	red wine	[236]
OTA	Fluorescence	CdTeQDs/TMPyP	98.9–102.2%	0.16 ng/mL	0.2–20 ng/mL	HT-2,ZEA,OTB,OTC	Astragalus membranaceus	[237]
OTA	Colorimetric	MnO2 nanosheet/AuNPs/ALP/AAP	99.4–104.2%	5 nM (2 μg/kg)	6.25–750 nM	ZeA,citrinin,TeA,AOH,ALT, AFB1,OTB	grape juice	[238]
OTA	Surface-enhanced Raman	AuAg NNSs/Fe_3O_4 MNPs/4-MBA/SER	92–112%	0.004 ng/mL	0.01–50 ng/mL	OTB,AFB1,ZEN,DON,FB1	red wine	[239]
OTA	SERS	Au@Ag NPs-Mxenes	93.31–97.44%	1.28 pM	0.10–10 nM	BSA, AFB1, FB1, MC-LR	red wine	[240]
OTA	Impedimetric	Au electrode/BSA/nanogold	90.56–104.2%	0.03 ng/mL	0.1–10 ng/mL	N-acetyl-L-phenylalanine, warfarin	grapes	[241]
OTA	Fluorescence	Rnase H	96.1–107.5%	0.08 ng/mL	0.4 ng/mL	OTB, AFB1	red wine	[242]
OTA	Electrochemical	PEDOT-AuNFs/GOS/GCE	97.2–106.7%	4.9 pg/L	0.01–20 ng/L		wine	[243]
OTA	Fluorescence	AP@ MBs/cDNA	90–110%	0.63 ng/mL	1–1000 ng/mL	ZEA,OTB,AFB1	white/red wine, cereal drink, coffee/tea beverage	[244]

between 85.0 and 105.1%., and an impressive detection limit of 7.85 × 10^{-10} M [146].

As described above, aptamer based colorimetric assays could potentially find widespread application for on-site analysis, owing to its convenience of visual observation and simplicity [147,148], with gold nanoparticles (AuNPs) being attractive as labels due to their high extinction coefficient in the visible region and catalytic activity [149–151]. As can be seen in Fig. 7, Taghdisi et al., proposed a colorimetric aptasensor for the determination of ZEN exploiting the catalytic performance of AuNPs with Exonuclease III-assisted signal amplification, achieving a dynamic range from 20 to 80000 ng/L, with a limit of detection for ZEN of 10 ng/L. The aptasensor was applied in human serum, with a detection limit of 40 ng/L, with recoveries in spiked serum samples in the range of 95–103% with relative standard deviations (RSDs) equal to or less than 7.1% [152].

Using a different approach, Wu et al. reported a sensitive up-conversion nanoparticles (UCNPs) and magnetic nanoparticles (MNPs)-based aptasensor for the quantitative detection of ZEN [153]. Hexagonal $NaYF_4$: 18 mol% Yb^{3+}, 2 mol% Er^{3+} UCNPs were synthesized using a facile hydrothermal methodology [154], and surface modification of UCNPs was performed based on the method described by Stöber, Fink, and Bohn [155] with minor modifications. MNPs were prepared by a modified co-precipitation method [156,157]. The luminescence bioassay platform was fabricated by immobilizing aptamer and its hybridized complementary strand (cDNA) onto the surfaces of MNPs and UCNPs, respectively, and then the aptamer-MNPs and cDNA-UCNPs were mixed to form the duplex structure. With the addition of the ZEN target, the ZEN aptamer was displaced from its complementary DNA, resulting in a decrease in the fluorescent intensity. The accuracy of the proposed aptamer-based bioassay for determining ZEN levels in real food samples was evaluated by detecting ZEN in spiked corn and beer samples, showing good recoveries from 93% to 110% [153]. Goud et al. used the same aptamer to develop an aptamer-based fluorescence quenching assay using exfoliated functional graphene oxide as a graphite nano powder [158,159], a highly efficient quencher, resulting in a concentration range of 0.5–64 ng/mL with a limit of detection of 0.5 ng/mL and the sensor was demonstrated to have very high selectivity. This aptasensor was successfully applied to the determination of ZEN in (spiked) alcoholic beverage samples, beer and wine, and recovery values in the range of 87–96% were obtained at levels as low as 1–16 ng/mL [160].

In another study, Niazi et al., reported a highly specific and sensitive ZEN recognition strategy based on time-resolved fluorescence, using Fe_3O_4 magnetic nanoparticles where the noise of the short-lived background fluorescence was eliminated by the long lifetime of the time-resolved NPs. Amine-functionalized magnetic nanoparticles (MNPs) functionalized with ZEN aptamers were used as a capture probe, whilst the signal probe was prepared by conjugating Ln^{3+}doped inorganic nanoparticles with complementary DNA [161]. $NaYF_4$: Ce/Tb NPs were prepared according to Tu's method [162] with some modifications and the $NaYF_4$: Ce/Tb NPs and MNPs were conjugated with avidin via glutaraldehyde [163]. The recovery ratio using wheat samples was between 90.04% and 114.75% and between 80.76% and 119.66% for maize samples [164].

In another approach, a time-resolved fluorometric aptasensor was described for the simultaneous detection of ZEN, T-2, and AFB1. Multicolor-emissive nanoparticles doped with lanthanide ions (Dy^{3+}, Tb^{3+}, Eu^{3+}) were functionalized with aptamers against the three targets. The aptamers adsorb onto tungsten disulfide (WS_2) nanosheets via van der Waals forces between nucleobases and the WS_2 basal plane, resulting in quenched fluorescence. In the presence of targets, fluorescence is restored due to interaction of the analyte with their respective aptamers, thus displacing them from the WS_2. The time-resolved fluorescence intensities at 488, 544 and 618 nm, corresponding to emissions of Dy^{3+}, Tb^{3+} and Eu^{3+} were used to quantify ZEN, T-2 and AFB1, respectively, with detection limits of 0.51, 0.33 and 0.40 pg/mL [165].

Table 2
Details of the properties of the aptamers detailed in this review.

Target	SELEX strategy	GC %	Kd (nM)	Structure	Ref.
Patulin	GO-SELEX	G-12% C-37%	21.83 ± 5.022	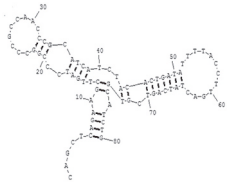	[51]
T-2 toxin	Magnetic beads/GO	G-27% C-17%	20.8 ± 3.1	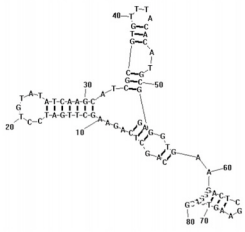	[69]
Aflatoxin B2		G-32% C-21%	No data		https://neoventures.ca/
Aflatoxin B2	Immuno affinity-SELEX	G-27% C-27%	AFLA53–48.29 ± 9.45	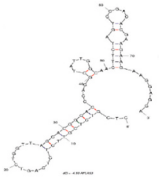	[80]
		G-55% C-10%	AFLA71–85.02 ± 25.74	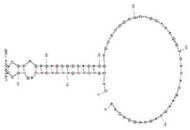	[80]
		G-35% C-12%	AFLA5-50.45 ± 11.06	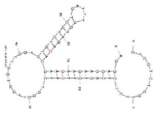	[80]
Aflatoxin B1	Magnetic beads combined with FluMag-SELEX, reverse SELEX	G-35% C-12%	11.39 ± 1.27	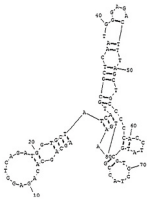	[207]
Zearalenone	Magnetic beads-SELEX	G-12% C-15%	41 ± 5	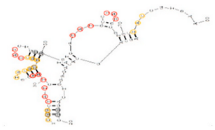	[146]
Fumonisin B1	Magnetic beads-SELEX	G-8% C-26%	100 ± 30		[171]
Ochratoxin	Resin affinity column	G-47% C-13%	200		[187]

In Han et al.'s work, a glassy carbon electrode (GCE) was covered by a graphene monologue, reduced molybdenum disulfide ($rMoS_2$) and gold nanoparticles coupled with the desired aptamer for each target (AP1 for ZEN and AP2 for FB1). The signals were further enhanced by the integration of Au NPs with the corresponding complementary DNA sequences (CP1 and CP2) of the aptamers via strong Au-SH and Au–NH_2 bonds. Thionine (Thi) and 6-(Ferrocenyl) hexanethiol (FC6S), displaying well-resolved reduction peaks at potentials of 0.24 V and 0.4 V,

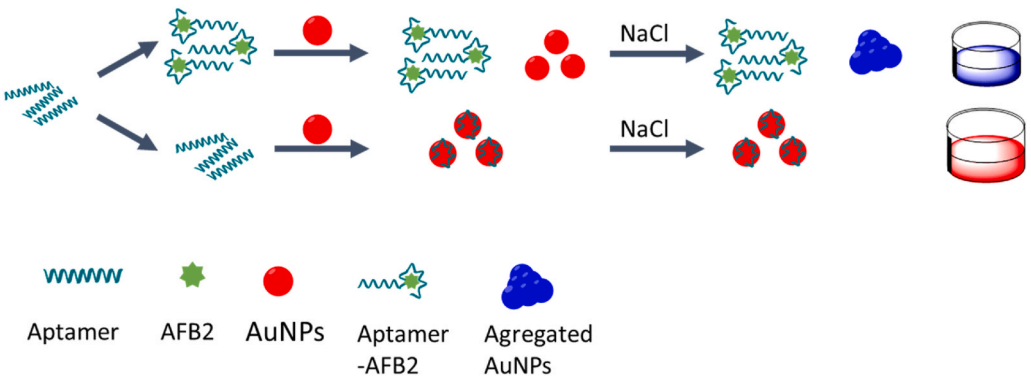

Fig. 6. Schematic diagram depicting the aptasensor for detecting AFB2 using AuNPs.

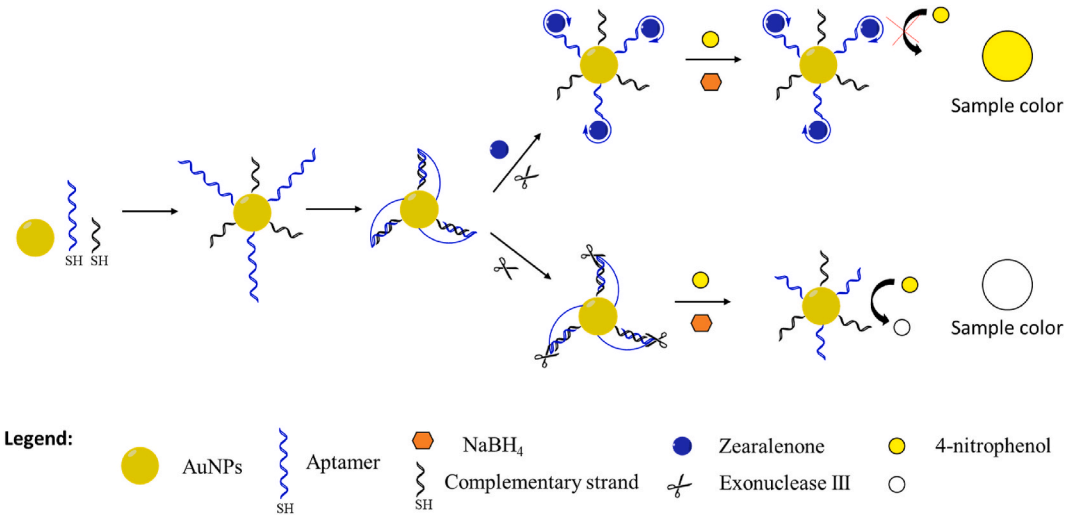

Fig. 7. Schematic representation of the colorimetric aptasensor for the detection of ZEN, based on the Exo III-assisted aptamer walker and catalytic reaction of AuNPs.

respectively, were added to the probes. The labeled CPs (L-CPs) including CP1–Au-Thi and CP2-Au-FC6S were bound to APs through complementary base pairing to form partially double-stranded DNA sequences, which could be displaced by the target molecules, thus resulting in signals proportional to the concentrations of the analytes [166].

Ji et al. also used GCEs, but this time modified with spherical Au-PANIAu nanohybrids to enhance the conductivity and immobilize more amino modified ZEN aptamer. L-glutamic acid (L-Glu) was used as precursor to obtain 3D sakura-shaped Cu@L-Glu MOCPs, which were combined with palladium-platinum nanoparticle (Pd-PtNPs) to obtain Cu@L-Glu/Pd-PtNPs nanocomposites which were used to label the complementary DNA (CP) (partially complementary with the ZEN aptamer) to form bio conjugates for signal amplification. Following hybridization with the ZEN aptamer and the Cu@L-Glu/Pd-PtNPs-CP, a dramatic decrease in the resistance was observed, confirming successful hybridization on the electrode surface. In the presence of ZEN, a significant reduction in signal was observed due to displacement of the aptamer. In addition, spherical Au-PANI-Au nanohybrids were used to modify the electrode, which further improved the sensitivity achieving a linear range from 1 fg/mL to 100 ng/mL and a limit of detection of 0.45 fg/mL [167].

A simple and sensitive aptamer-based lateral flow test strip for ZEN was successfully developed by Wu et al. [168] using the competitive format. Under the optimized conditions, the visual limit of detection of the strip was as low as 20 ng/mL, and the linear range was from 5 to 200 ng/mL with an assay time of 5 min. The specificity of the aptamer-based lateral flow strip was demonstrated using four different toxins: DON, OTA, FB1, and AFB1. Spiked corn samples containing ZEN at concentrations higher than 5 ng/mL demonstrated positive results, and the color intensity of the test line became weaker with increasing concentrations of ZEN. The aptamer-based test strip was stable for 2 months [168].

2.6. *Fumonisins B1*

Fumonisin B1 (FB1) is part of fumonisins family, which are toxins mostly produced by several species of Fusarium molds, such as *Fusarium verticillioides* and *F. proliferatum* [169] and occurs mainly in maize, wheat and other cereals. Human exposure occurs at levels of micrograms to milligrams per day and is greatest in regions where maize products are the dietary staple. As with the other mycotoxins, the currently accepted testing methods of FB1 in maize rely on the use of chromatography-based confirmatory methods and immunoassays, with enzyme-linked immunosorbent assay (ELISA) as the most popular method [170].

McKeague et al. [171] successfully selected an aptamer against FB1 with a dissociation constant of 100 ± 30 nM, and various aptamer based tools exploiting this aptamer have been reported.

Upconversion nanoparticles convert near infrared radiations into visible wavelengths via a nonlinear optical process known as photon upconversion [172], and Wu et *al.* presented an aptasensor for FB1

[173], based on duplex fluorescence quenching [174] of the multicolor upconversion fluorescent nanoparticles by GO (Fig. 8). The 2 different UCNPs were synthesized and functionalized with immobilized OTA-aptamer and FB1 aptamer. As previously explained, aptamer is bound to GO, and in the absence of the target there is a quenching of fluorescence of the aptamer modified UCNPs. In the presence of both targets, OTA and FB1, the aptamer binds to the target, and is thus not quenched by the GO, achieving a detection limit of 0.1–500 ng/mL.

He et al. [175] group combined both surface-enhanced Raman spectroscopy (SERS) and fluorimetry. In the absence of FB1, fluorophore-labeled aptamer hybridizes with cDNA immobilized on the surface of platinum-coated gold nanorod (AuNR). As a result, strong SERS and weak fluorescence signals are obtained. In the presence of FB1, the aptamer is displaced from its cDNA, the fluorescence increases, while the SERS signal is decreased. This approach is a double control and reduces the risk of false-positive or false-negative results. The limit of detection achieved was 0.25 ng/mL.

Wang et al. [176] developed a FRET aptasensor for the simultaneous determination of AFB1 and FB1 levels using quantum dots with different emission peaks (GQDs and RQDs) and magnetic GO/Fe_3O_4 as the single acceptor. The principle is the same as in previously described papers, with the only difference being the use of GO/Fe_3O_4, which can be effectively removed via magnetic separation to eliminate the background interference. Fluorescence recovery was achieved simultaneously in the presence of AFB1 and FB1. The limit of detection was 0.0162 ng/mL [176].

An aptasensor for the simultaneous recognition of FB1 and OTA based on time-resolved fluorescence nanoparticles (TRF-NPs); $NaYF_4$: Ce,Tb and NH_2-Eu/DPA@SiO_2 nanoparticles and magnetic nanoparticles (MNPs) (Fig. 9) has been reported. Biotinylated aptamers for FB1 and OTA are immobilized on avidin coated magnetic nanoparticles, while cDNA is attached to TRF-NPs. In the absence of the targets, the biocomplex of MNPs-aptamers/TRF-NPs-cDNA is assembled through hybridization of aptamer and cDNA, while, in the presence of FB1 and OTA, the partially complementary DNA is displaced from the aptamer, therefore liberating some TRF-NPs-cDNA, leading to decrease in fluorescent signal. The detection limit for this assay is 0.019 pg/mL for FB1 and 0.015 pg/mL for OTA [177].

Another group, Yue et al. [178] developed a different technique, based on the use of an aptamer–photonic crystal encoded suspension array. They used aptamers against OTA and FB1, which were immobilized on the surfaces of photonic crystals via chemical bonding. The fluorescence-labeled complementary DNA of the aptamer is displaced when the target mycotoxins appear in a sample, resulting in a decrease in fluorescence intensity of the microsphere. The difference value of fluorescent intensities for each kind of silica photonic crystal microsphere (SPCM) quantitatively conveys the concentration of mycotoxin, and the structure colors or reflectance peak positions of the SPCMs confirm the kind of mycotoxin detected.

2.7. Ochratoxin A

Ochratoxin A (OTA), an ubiquitous mycotoxin, is produced by various species of *Aspergillus* and *Penicillium*. Likely, it can contaminate cereals (wheat, corn, barely) and wines [179–181]. Several studies have introduced OTA as a nephrotoxic, hepatotoxic, neurotoxic, immunotoxin, and teratogenic agent [180]. Several methods have been developed to detect OTA including mass spectroscopy [182,183], high performance chromatography [31,184],and antibody based techniques [185,186].

In 2008, the first aptamer for OTA was selected Cruz-Aguado et al. [187] using a resin affinity column. Using equilibrium dialysis the selected aptamer was examined for the binding to OTA and the best aptamer candidate had a K_d equal to 0.2 μM. The authors demonstrated the specificity via evaluation of the interaction of the selected aptamer with warfarin, a hydrophobic molecule with a similar structure to OTA, NAP (N-acetyl-L-phenylalanine) and OTB, a structural analogue of OTA that lacks the chlorine atom in the isocoumarin ring. They also highlighted that binding of OTA to the DNA aptamers depended on the presence of the Mg^{2+} and Ca^{2+} divalent cations. To demonstrate the potential use of the aptamers in the quantitative determination of OTA in agricultural commodities the authors went further in their study in detection of OTA in wheat grains. The high specificity of the aptamer affinity column to OTA allowed the direct determination of OTA by its fluorescence with no need for other separation methods, as all other fluorescent contaminants were removed during the washing steps. This aptamer exhibited the highest affinity and specificity towards OTA and as result this has been widely exploited in a variety of aptasensor formats, as detailed in a previously published review [188]. Since the publication of that review, there have been new reports of aptasensors, which have been included in Table 1.

3. Conclusion and discussion

Mycotoxins are secondary metabolites produced by fungi and can easily enter the food chain. The carcinogenic properties of mycotoxins threaten our daily life through the food supply. They show a serious risk to humans and animals, leading to diarrhea, lethargy, weight loss, immune suppression, necrosis, apoptosis, cancer and even death. Different laboratory techniques such as high-performance liquid chromatography and gas chromatography, along with fluorescent detectors or mass spectrometry detectors have been applied for mycotoxin detection. Antibodies are also implemented for the detection of mycotoxins, however, lately aptamers have garnered increasing attention.

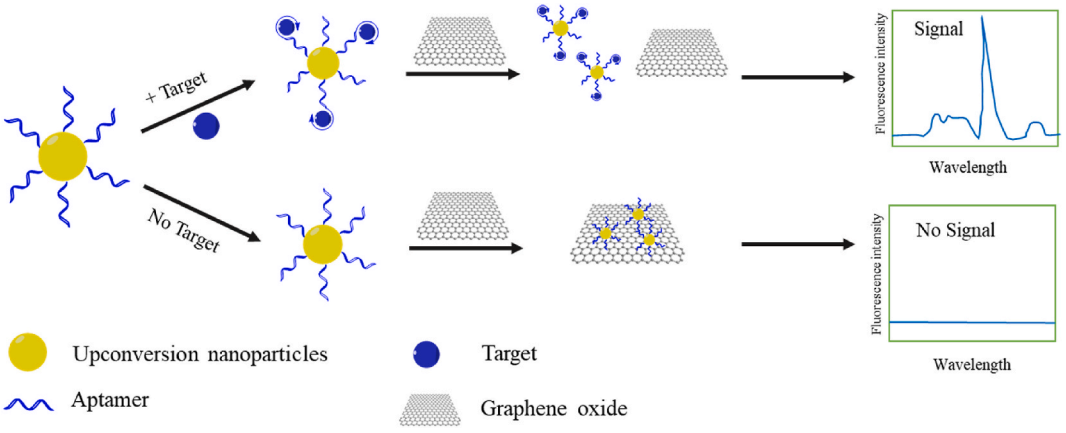

Fig. 8. Illustration of the multiplexed upconversion fluorescence quenching of the UCNPs by GO.

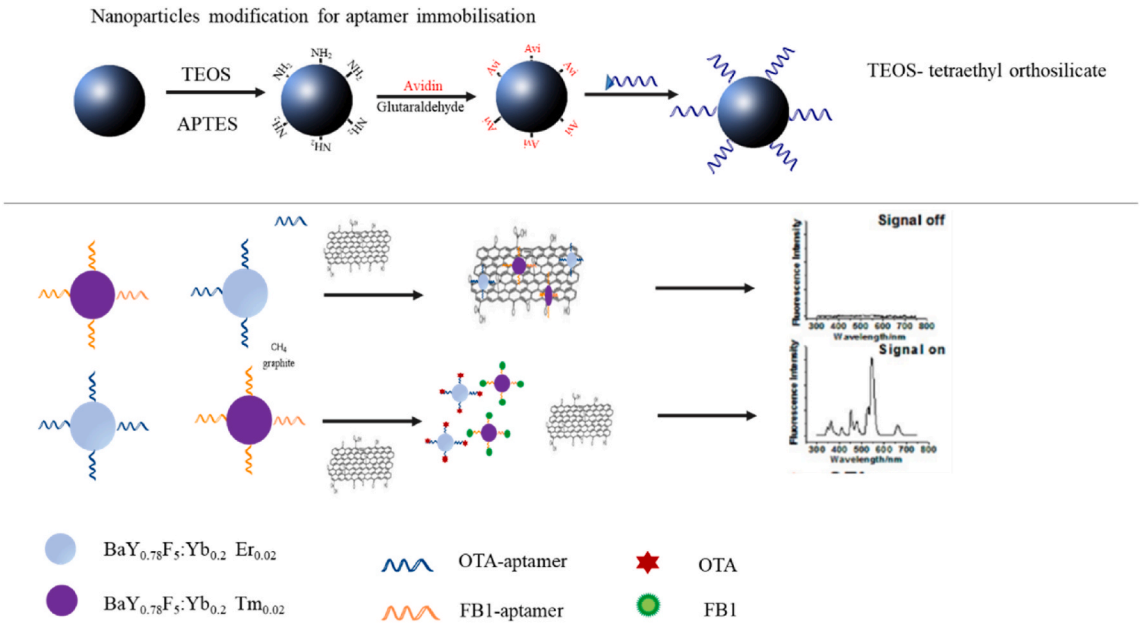

Fig. 9. Illustration for simultaneous recognition of mycotoxin using time resolved fluorescence NPs as labels.

Aptamers are good alternatives to replace antibodies in the development of point of need devices due to their outstanding properties. The main advantages include their ability to detect small molecules, stability, versatility, ease of manufacture, reversibility of the binding, reusability, batch to batch reproducibility, markedly lower price and an avoidance of animal hosts.

Due to the mentioned properties, they have been used to develop different types of aptasensors based on various different detection techniques, including electrochemical (differential pulse voltammetry, square wave voltammetry, impedance), optical (Raman, fluorescence, SPR) as well as lateral flow assays.

The aptasensors presented in this review are highly selective and reproducible for the detection of mycotoxins in real samples, and most of them were designed for single mycotoxin detection and a few of them for duplex or triplex detection. Examples of this include the combined detection of FB1 and OTA detection based on duplex fluorescence quenching or detection of ZEN, FB1 and OTA using a combination of SERS and fluorimetry.

Each of the techniques have advantages and disadvantages. Electrochemical aptasensors require simple instrumentation, are compatible with micro fabrication and miniaturization and they have high sensitivity. Whilst most electrochemical aptasensors require immobilization of the aptamer on a solid substrate, optical methods are also compatible with aptamers in solution. Methods that have the aptamers in solution are in general simpler than those where the aptamer is immobilized on a surface, however, if aptamers are in solution they are discarded together with the analyzed samples, limiting their reusability. On the other hand, lateral flow, as a user-friendly method, normally requires low sample manipulation and provides a visual answer in a short interval of time. The successful commercial implementation of aptasensors has yet to be achieved but they do have huge potential for the fast, accurate and high-performance detection of toxins in monitoring programs.

Acknowledgements

The authors are grateful to King Abdulaziz University (Saudi Arabia) for financing the collaborative project “Cost-effective tools for mycotoxin testing”.

References

[1] J.L. Richard, Some major mycotoxins and their mycotoxicoses-An overview, Int, J. Food Microbiol (2007), https://doi.org/10.1016/j.ijfoodmicro.2007.07.019.
[2] H. Hussein, J. Brasel, Toxicity, metabolism and impact of mycotoxins on human and animals, Toxicology (2001), https://doi.org/10.1016/S0300-483X(01)00471-1.
[3] C.P. Wild, Y.Y. Gong, Mycotoxins and human disease: a largely ignored global health issue, Carcinogenesis (2009), https://doi.org/10.1093/carcin/bgp264.
[4] F. Wu, Measuring the economic impacts of Fusarium toxins in animal feeds, Anim. Feed Sci, Technol. (2007), https://doi.org/10.1016/j.anifeedsci.2007.06.010.
[5] W.L. Bryden, Mycotoxin contamination of the feed supply chain: implications for animal productivity and feed security, Anim. Feed Sci, Technol. (2012), https://doi.org/10.1016/j.anifeedsci.2011.12.014.
[6] F. Wu, Global impacts of aflatoxin in maize: trade and human health, World Mycotoxin J (2015), https://doi.org/10.3920/WMJ2014.1737.
[7] G. Pulina, G. Battacone, G. Brambilla, F. Cheli, P.P. Danieli, F. Masoero, A. Pietri, B. Ronchi, An update on the safety of foods of animal origin and feeds, Ital, J. Anim. Sci. (2014), https://doi.org/10.4081/ijas.2014.3571.
[8] L. Pinotti, M. Ottoboni, C. Giromini, V. Dell'Orto, F. Cheli, Mycotoxin contamination in the EU feed supply chain: a focus on Cereal Byproducts, Toxins, Basel, 2016, https://doi.org/10.3390/TOXINS8020045.
[9] R. Ghali, K. Hmaissia-khlifa, H. Ghorbel, K. Maaroufi, A. Hedili, Incidence of aflatoxins, ochratoxin A and zearalenone in tunisian foods, Food Contr. (2008), https://doi.org/10.1016/j.foodcont.2007.09.003.
[10] E.M. Binder, L.M. Tan, L.J. Chin, J. Handl, J. Richard, Worldwide occurrence of mycotoxins in commodities, feeds and feed ingredients, Anim. Feed Sci, Technol. (2007), https://doi.org/10.1016/j.anifeedsci.2007.06.005.
[11] S. Marin, A.J. Ramos, G. Cano-Sancho, V. Sanchis, Mycotoxins: occurrence, toxicology, and exposure assessment, Food Chem. Toxicol. (2013), https://doi.org/10.1016/j.fct.2013.07.047.
[12] I. Rodrigues, K. Naehrer, A three-year survey on the worldwide occurrence of mycotoxins in feedstuffs and feed, Toxins, Basel, 2012, https://doi.org/10.3390/toxins4090663.
[13] E. Streit, G. Schatzmayr, P. Tassis, E. Tzika, D. Marin, I. Taranu, C. Tabuc, A. Nicolau, I. Aprodu, O. Puel, I.P. Oswald, Current situation of mycotoxin contamination and co-occurrence in animal feed–focus on Europe, Toxins, Basel, 2012, https://doi.org/10.3390/toxins4100788.
[14] E. Streit, K. Naehrer, I. Rodrigues, G. Schatzmayr, Mycotoxin occurrence in feed and feed raw materials worldwide: long-term analysis with special focus on Europe and Asia, J. Sci. Food Agric. (2013), https://doi.org/10.1002/jsfa.6225.
[15] M. De Boevre, J.D. Di Mavungu, S. Landschoot, K. Audenaert, M. Eeckhout, P. Maene, G. Haesaert, S. De Saeger, Natural occurrence of mycotoxins and their masked forms in food and feed products, World Mycotoxin J. (2012), https://doi.org/10.3920/WMJ2012.1410.
[16] V.L. Pereira, J.O. Fernandes, S.C. Cunha, Mycotoxins in cereals and related foodstuffs: a review on occurrence and recent methods of analysis, Trends Food Sci. Technol. (2014), https://doi.org/10.1016/j.tifs.2014.01.005.
[17] W. Hu, X. Li, G. He, Z. Zhang, X. Zheng, P. Li, C.M. Li, Sensitive competitive immunoassay of multiple mycotoxins with non-fouling antigen microarray, Biosens, Bioelectron (2013), https://doi.org/10.1016/j.bios.2013.06.037.

[18] D. Guan, P. Li, Q. Zhang, W. Zhang, D. Zhang, J. Jiang, An ultra-sensitive monoclonal antibody-based competitive enzyme immunoassay for aflatoxin M1 in milk and infant milk products, Food Chem. (2011), https://doi.org/10.1016/j.foodchem.2010.10.006.
[19] X. Tang, X. Li, P. Li, Q. Zhang, R. Li, W. Zhang, X. Ding, J. Lei, Z. Zhang, Development and application of an immunoaffinity column enzyme immunoassay for mycotoxin zearalenone in complicated samples, PloS One (2014), https://doi.org/10.1371/journal.pone.0085606.
[20] N.V. Beloglazova, P.S. Shmelin, I.Y. Goryacheva, S. De Saeger, Liposomes loaded with quantum dots for ultrasensitive on-site determination of aflatoxin M1 in milk products Rapid Detection in Food and Feed, Anal. Bioanal. Chem. (2013), https://doi.org/10.1007/s00216-013-7096-6.
[21] Z.R. Fang Fang, Zhang Xu, Determination of aflatoxin in cereal by immune-affinity column clean-up and HPLC-FLD with post-column photochemical derivation, Cereal & Feed Ind. (2012).
[22] F. Shi, J. Liu, Determination of aflatoxin B1 in edible vegetable oil by immunoaffinity column purification and HPLC-MS/MS, China Oils Fats (2014).
[23] H. Sharma, R. Mutharasan, Review of biosensors for foodborne pathogens and toxins, Sensor. Actuator. B Chem. (2013), https://doi.org/10.1016/j.snb.2013.03.137.
[24] C.M. Maragos, Biosensors for mycotoxin analysis: recent developments and future prospects, World Mycotoxin J. (2009), https://doi.org/10.3920/wmj2008.1117.
[25] X. Guo, F. Wen, N. Zheng, Q. Luo, H. Wang, H. Wang, S. Li, J. Wang, Development of an ultrasensitive aptasensor for the detection of aflatoxin B1, Biosens. Bioelectron. (2014), https://doi.org/10.1016/j.bios.2014.01.045.
[26] L. Anfossi, C. Baggiani, C. Giovannoli, G. D'Arco, G. Giraudi, Lateral-flow immunoassays for mycotoxins and phycotoxins: A review, Anal. Bioanal. Chem (2013), https://doi.org/10.1007/s00216-012-6033-4.
[27] X. Chen, Y. Huang, X. Ma, F. Jia, X. Guo, Z. Wang, Impedimetric aptamer-based determination of the mold toxin fumonisin B1, Microchim. Acta (2015), https://doi.org/10.1007/s00604-015-1492-x.
[28] Q. Li, Z. Lu, X. Tan, X. Xiao, P. Wang, L. Wu, K. Shao, W. Yin, H. Han, Ultrasensitive detection of aflatoxin B1by SERS aptasensor based on exonuclease-assisted recycling amplification, Biosens, Bioelectron (2017), https://doi.org/10.1016/j.bios.2017.05.031.
[29] C. Zhu, G. Zhang, Y. Huang, S. Yang, S. Ren, Z. Gao, A. Chen, Dual-competitive lateral flow aptasensor for detection of aflatoxin B1in food and feedstuffs, J. Hazard Mater. (2018), https://doi.org/10.1016/j.jhazmat.2017.10.026.
[30] C. Tuerk, L. Gold, Systematic evolution of ligands by exponential enrichment: RNA ligands to bacteriophage T4 DNA polymerase, Science 84 (1990), https://doi.org/10.1126/science.2200121.
[31] M. Blank, M. Blind, Aptamers as tools for target validation, Curr, Opin. Chem. Biol (2005), https://doi.org/10.1016/j.cbpa.2005.06.011.
[32] A.D. Ellington, J.W. Szostak, Selection in vitro of single-stranded DNA molecules that fold into specific ligand-binding structures, Nature (1992), https://doi.org/10.1038/355850a0.
[33] J.C. Cox, A.D. Ellington, Automated selection of anti-protein aptamers, Bioorg. Med. Chem. (2001). https://doi.org/10.1016/s0968-0896(01)00028-1.
[34] M. Berezovski, M. Musheev, A. Drabovich, S.N. Krylov, Non-SELEX selection of aptamers, J. Am. Chem. Soc. (2006), https://doi.org/10.1021/ja056943j.
[35] H. Sun, X. Zhu, P.Y. Lu, R.R. Rosato, W. Tan, Y. Zu, Oligonucleotide aptamers: new tools for targeted cancer therapy, Mol. Ther. Nucleic Acids (2014), https://doi.org/10.1038/mtna.2014.32.
[36] S.D. Jayasena, Aptamers: an emerging class of molecules that rival antibodies in diagnostics, Clin, Inside Chem. (1999), https://doi.org/10.1038/mtna.2014.74.
[37] Z. Cao, R. Tong, A. Mishra, W. Xu, G.C.L. Wong, J. Cheng, Y. Lu, Reversible cell-specific drug delivery with aptamer-functionalized liposomes, Angew, in: Chemie - Int (Ed.), 2009, https://doi.org/10.1002/anie.200901452.
[38] C.S.M. Ferreira, M.C. Cheung, S. Missailidis, S. Bisland, J. Gariépy, Phototoxic aptamers selectively enter and kill epithelial cancer cells, Nucleic Acids Res. (2009), https://doi.org/10.1093/nar/gkn967.
[39] J.W. Bennett, M. Klich, M. Mycotoxins, Mycotoxins, clin. Microbiol. Rev. https://doi.org/10.1128/CMR.16.3.497, 2003.
[40] M.M. Moake, O.I. Padilla-Zakour, R.W. Worobo, Comprehensive review of patulin control methods in foods, Compr. Rev. Food Sci. Food Saf. (2005), https://doi.org/10.1111/j.1541-4337.2005.tb00068.x.
[41] M.I. Luque, A. Rodríguez, M.J. Andrade, R. Gordillo, M. Rodríguez, J.J. Córdoba, Development of a PCR protocol to detect patulin producing moulds in food products, Food Contr. (2011), https://doi.org/10.1016/j.foodcont.2011.04.020.
[42] P.M. Scott, J.W. Lawrence, W. Van Walbeek, NOTES detection of mycotoxins by thin-layer chromatography: application to screening of fungal extracts, appl, Microbiol. (1970).
[43] G.S. Shephard, N.L. Leggott, Chromatographic determination of the mycotoxin patulin in fruit and fruit juices, J. Chromatogr. A (2000), https://doi.org/10.1016/S0021-9673(99), 01341–01342.
[44] M. Seo, B. Kim, S.Y. Baek, An optimized method for the accurate determination of patulin in apple products by isotope dilution-liquid chromatography/mass spectrometry, Anal. Bioanal, Inside Chem. (2015), https://doi.org/10.1007/s00216-015-8705-3.
[45] E. Beltrán, M. Ibáñez, J.V. Sancho, F. Hernández, Determination of patulin in apple and derived products by uhplc-ms/ms, Study of matrix effects with atmospheric pressure ionisation sources, Food Chem (2014), https://doi.org/10.1016/j.foodchem.2013.07.069.
[46] N.H. Schebb, H. Faber, R. Maul, F. Heus, J. Kool, H. Irth, U. Karst, Analysis of glutathione adducts of patulin by means of liquid chromatography (HPLC) with biochemical detection (BCD) and electrospray ionization tandem mass spectrometry (ESI-MS/MS), Anal. Bioanal. Chem. (2009), https://doi.org/10.1007/s00216-009-2765-1.
[47] Y. Wang, Z. Li, T.J. Weber, D. Hu, C.T. Lin, J. Li, Y. Lin, In situ live cell sensing of multiple nucleotides exploiting DNA/RNA aptamers and graphene oxide nanosheets, Anal, Inside Chem. (2013), https://doi.org/10.1021/ac400858g.
[48] P. Zhang, Y. Wang, F. Leng, Z.H. Xiong, C.Z. Huang, Highly selective and sensitive detection of coralyne based on the binding chemistry of aptamer and graphene oxide, Talanta (2013), https://doi.org/10.1016/j.talanta.2013.03.013.
[49] D. Chen, H. Feng, J. Li, Graphene oxide: preparation, functionalization, and electrochemical applications, Chem. Rev. (2012), https://doi.org/10.1021/cr300115g.
[50] C. Chung, Y.K. Kim, D. Shin, S.R. Ryoo, B.H. Hong, D.H. Min, Biomedical applications of graphene and graphene oxide, Acc. Chem. Res. (2013), https://doi.org/10.1021/ar300159f.
[51] S. Wu, N. Duan, W. Zhang, S. Zhao, Z. Wang, Screening and development of DNA aptamers as capture probes for colorimetric detection of patulin, Anal. Biochem. (2016), https://doi.org/10.1016/j.ab.2016.05.024.
[52] J.W. Park, R. Tatavarty, D.W. Kim, H.T. Jung, M.B. Gu, Immobilization-free screening of aptamers assisted by graphene oxide, Chem. Commun. (2012), https://doi.org/10.1039/c2cc16473f.
[53] X.D. Baoshan He, Aptamer based voltammetric patulin assay based on the use of ZnO nanorods, 2018.
[54] R. Khan, S. Ben Aissa, T.A. Sherazi, G. Catanante, A. Hayat, J.L. Marty, Development of an impedimetric aptasensor for label free detection of patulin in apple juice, Molecules (2019), https://doi.org/10.3390/molecules24061017.
[55] K. Abnous, N.M. Danesh, M. Ramezani, P. Lavaee, S.H. Jalalian, R. Yazdian-Robati, A.S. Emrani, K.Y. Hassanabad, S.M. Taghdisi, A novel aptamer-based DNA diamond nanostructure for in vivo targeted delivery of epirubicin to cancer cells, RSC Adv. (2017), https://doi.org/10.1039/c6ra28234b.
[56] L. Ma, T. Guo, S. Pan, Y. Zhang, A fluorometric aptasensor for patulin based on the use of magnetized graphene oxide and DNase I-assisted target recycling amplification, Microchim. Acta (2018), https://doi.org/10.1007/s00604-018-3023-z.
[57] A. Ahmadi, N.M. Danesh, M. Ramezani, M. Alibolandi, P. Lavaee, A.S. Emrani, K. Abnous, S.M. Taghdisi, A rapid and simple ratiometric fluorescent sensor for patulin detection based on a stabilized DNA duplex probe containing less amount of aptamer-involved base pairs, Talanta (2019), https://doi.org/10.1016/j.talanta.2019.06.057.
[58] Y. Li, Z. Wang, R.C. Beier, J. Shen, D. De Smet, S. De Saeger, S. Zhang, T-2 toxin, a trichothecene mycotoxin: review of toxicity, metabolism, and analytical methods, J. Agric. Food Chem. (2011), https://doi.org/10.1021/jf200767q.
[59] M. Pascale, G. Panzarini, A. Visconti, Determination of HT-2 and T-2 toxins in oats and wheat by ultra-performance liquid chromatography with photodiode array detection, Talanta (2012), https://doi.org/10.1016/j.talanta.2011.12.017.
[60] L. Sibanda, S. De Saeger, C. Van Peteghem, J. Grabarkiewicz-Szczesna, M. Tomczak, Detection of T-2 toxin in different cereals by flow-through enzyme immunoassay with a simultaneous internal reference, J. Agric. Food Chem. (2000), https://doi.org/10.1021/jf000337k.
[61] H.J. van der Fels-Klerx, Occurrence data of trichothecene mycotoxins T-2 toxin and HT-2 toxin in food and feed, Sci. Rep. Submitt. to EFSA (2010), https://doi.org/10.2903/sp.efsa.2010.EN-66.
[62] S.C. on Food, Opinion of the scientific committee on food on Fusarium toxins. Part 6: Group evaluation of T-2 toxin, HT-2 toxin, nivalenol and deoxynivalenol, n.d.
[63] M.F. Raisbeck, G.E. Rottinghaus, J.D. Kendall, Effects of naturally occurring mycotoxins on ruminants, Mycotoxins Anim. Foods 1991 (1991) 647–677.
[64] Y. Li, X. Luo, S. Yang, X. Cao, Z. Wang, W. Shi, S. Zhang, High specific monoclonal antibody production and development of an ELISA method for monitoring T-2 toxin in rice, J. Agric. Food Chem. (2014), https://doi.org/10.1021/jf404818r.
[65] Y. Sun, G. Zhang, H. Zhao, J. Zheng, F. Hu, B. Fang, Liquid chromatography-tandem mass spectrometry method for toxicokinetics, tissue distribution, and excretion studies of T-2 toxin and its major metabolites in pigs, J. Chromatogr. B Anal. Technol. Biomed. Life Sci (2014), https://doi.org/10.1016/j.jchromb.2014.03.010.
[66] F. Soleimany, S. Jinap, A. Faridah, A. Khatib, A UPLC-MS/MS for simultaneous determination of aflatoxins, ochratoxin A, zearalenone, DON, fumonisins, T-2 toxin and HT-2 toxin, in cereals, Food Contr. (2012), https://doi.org/10.1016/j.foodcont.2011.11.012.
[67] M. Kong, W. Zhang, X. Shen, H. Yang, Z. Yang, Validation of a gas chromatography−electron capture detection of T-2 and HT-2 toxins in Chinese herbal medicines and related products after immunoaffinity column clean-up and pre-column derivatization, Food Chem. (2012).
[68] N. Ramakrishna, J. Lacey, A.A.G. Candlish, J.E. Smith, I.A. Goodbrand, Monoclonal antibody-based enzyme linked immunosorbent assay of aflatoxin B1, T-2 toxin, and ochratoxin A in barley, J. Assoc. Off. Anal. Chem (1990).
[69] X. Chen, Y. Huang, N. Duan, S. Wu, Y. Xia, X. Ma, C. Zhu, Y. Jiang, Z. Wang, Screening and identification of DNA aptamers against T-2 toxin assisted by graphene oxide, J. Agric. Food Chem. (2014), https://doi.org/10.1021/jf5032058.
[70] H. Zhong, C. Yu, R. Gao, J. Chen, Y. Yu, Y. Geng, Y. Wen, J. He, A novel sandwich aptasensor for detecting T-2 toxin based on rGO-TEPA-Au@Pt nanorods with a dual signal amplification strategy, Biosens. Bioelectron. (2019), https://doi.org/10.1016/j.bios.2019.111635.
[71] I.M. Khan, S. Zhao, S. Niazi, A. Mohsin, M. Shoaib, N. Duan, S. Wu, Z. Wang, Silver nanoclusters based FRET aptasensor for sensitive and selective fluorescent

detection of T-2 toxin, Sensor. Actuator. B Chem. (2018), https://doi.org/10.1016/j.snb.2018.09.021.
[72] J. Yu, Current understanding on aflatoxin biosynthesis and future perspective in reducing aflatoxin contamination, Toxins, Basel, 2012, https://doi.org/10.3390/toxins4111024.
[73] Iarc monographs on the evaluation of carcinogenic risks to humans, IARC monogr. Eval. Carcinog. Risks to humans. https://doi.org/10.1136/jcp.48.7.691-a, 2010.
[74] S. Tabata, H. Kamimura, A. Ibe, H. Hashimoto, M. Iida, Y. Tamura, T. Nishima, Aflatoxin contamination in foods and foodstuffs in Tokyo: 1986-1990., J. AOAC Int (1993), https://doi.org/10.3358/shokueishi.39.6_444.
[75] S. Bakirdere, S. Bora, E.G. Bakirdere, F. Aydin, Y. Arslan, O.T. Komesli, I. Aydin, E. Yildirim, Aflatoxin species: their health effects and determination methods in different foodstuffs, Cent. Eur. J. Chem. (2012), https://doi.org/10.2478/s11532-012-0009-2.
[76] N. Mahnine, G. Meca, A. Elabidi, M. Fekhaoui, A. Saoiabi, G. Font, J. Mañes, A. Zinedine, Further data on the levels of emerging Fusarium mycotoxins enniatins (A, A1, B, B1), beauvericin and fusaproliferin in breakfast and infant cereals from Morocco, Food Chem. (2011), https://doi.org/10.1016/j.foodchem.2010.06.058.
[77] V.S. Sobolev, J.W. Dorner, Cleanup procedure for determination of aflatoxins in major agricultural commodities by liquid chromatography, J. AOAC Int. (2002) 33003–33006, https://doi.org/10.1016/S1059-4337(4.
[78] D. Saha, D. Acharya, D. Roy, D. Shrestha, T.K. Dhar, Simultaneous enzyme immunoassay for the screening of aflatoxin B1 and ochratoxin A, in chili samples, Anal. Chim. Acta (2007), https://doi.org/10.1016/j.aca.2006.11.042.
[79] X. Ma, W. Wang, X. Chen, Y. Xia, N. Duan, S. Wu, Z. Wang, Selection, characterization and application of aptamers targeted to Aflatoxin B2, Food Contr. (2015), https://doi.org/10.1016/j.foodcont.2014.07.037.
[80] K. Setlem, B. Mondal, S. Ramlal, J. Kingston, Immuno affinity SELEX for simple, rapid, and cost-effective aptamer enrichment and identification against aflatoxin B1, Front. Microbiol. (2016), https://doi.org/10.3389/fmicb.2016.01909.
[81] G.S. Geleta, Z. Zhao, Z. Wang, A novel reduced graphene oxide/molybdenum disulfide/polyaniline nanocomposite-based electrochemical aptasensor for detection of aflatoxin B1, Analyst (2018), https://doi.org/10.1039/c7an02050c.
[82] G. Peng, X. Li, F. Cui, Q. Qiu, X. Chen, H. Huang, Aflatoxin B1 electrochemical aptasensor based on tetrahedral DNA nanostructures functionalized three dimensionally ordered macroporous MoS2-AuNPs film, ACS Appl. Mater. Interfaces (2018), https://doi.org/10.1021/acsami.8b01693.
[83] K. Abnous, N.M. Danesh, M. Alibolandi, M. Ramezani, A. Sarreshtehdar Emrani, R. Zolfaghari, S.M. Taghdisi, A new amplified π-shape electrochemical aptasensor for ultrasensitive detection of aflatoxin B1, Biosens. Bioelectron. (2017), https://doi.org/10.1016/j.bios.2017.03.028.
[84] W. Zheng, J. Teng, L. Cheng, Y. Ye, D. Pan, J. Wu, F. Xue, G. Liu, W. Chen, Hetero-enzyme-based two-round signal amplification strategy for trace detection of aflatoxin B1 using an electrochemical aptasensor, Biosens, Bioelectron (2016), https://doi.org/10.1016/j.bios.2016.01.091.
[85] C. Wang, J. Qian, K. An, C. Ren, X. Lu, N. Hao, Q. Liu, H. Li, X. Huang, K. Wang, Fabrication of magnetically assembled aptasensing device for label-free determination of aflatoxin B1 based on EIS, Biosens. Bioelectron. (2018), https://doi.org/10.1016/j.bios.2018.02.043.
[86] J. Homola, S.S. Yee, G. Gauglitz, Surface plasmon resonance sensors: review, Sensors Actuators, Biol. Chem. (1999), https://doi.org/10.1016/S0925-4005(98), 00321–00329.
[87] Y. Wang, B. Yan, L. Chen, SERS Tags: novel optical nanoprobes for bioanalysis, Chem. Rev. (2013), https://doi.org/10.1021/cr300120g.
[88] J.F. Li, J.R. Anema, T. Wandlowski, Z.Q. Tian, Dielectric shell isolated and graphene shell isolated nanoparticle enhanced Raman spectroscopies and their applications, Chem. Soc. Rev. (2015), https://doi.org/10.1039/c5cs00501a.
[89] J. Ando, M. Asanuma, K. Dodo, H. Yamakoshi, S. Kawata, K. Fujita, M. Sodeoka, Alkyne-tag SERS screening and identification of small-molecule-binding sites in protein, J. Am. Chem. Soc. (2016), https://doi.org/10.1021/jacs.6b06003.
[90] Y. Cui, X.S. Zheng, B. Ren, R. Wang, J. Zhang, N.S. Xia, Z.Q. Tian, Au@organosilica multifunctional nanoparticles for the multimodal imaging, Chem. Sci. (2011), https://doi.org/10.1039/c1sc00242b.
[91] J. Zhang, L. He, P. Chen, C. Tian, J. Wang, B. Liu, C. Jiang, Z. Zhang, A silica-based SERS chip for rapid and ultrasensitive detection of fluoride ions triggered by a cyclic boronate ester cleavage reaction, Nanoscale (2017), https://doi.org/10.1039/c6nr07545b.
[92] D.P. Dos Santos, M.L.A. Temperini, A.G. Brolo, Single-molecule surface-enhanced (resonance) Raman scattering (SE(R)RS) as a probe for metal colloid aggregation state, J. Phys. Chem. C (2016), https://doi.org/10.1021/acs.jpcc.6b02400.
[93] W. Wang, W. Wang, L. Liu, L. Xu, H. Kuang, J. Zhu, C. Xu, Nanoshell-enhanced Raman spectroscopy on a microplate for staphylococcal enterotoxin B sensing, ACS Appl. Mater. Interfaces (2016), https://doi.org/10.1021/acsami.6b02905.
[94] W. Wu, Z. Zhu, B. Li, Z. Liu, L. Jia, L. Zuo, L. Chen, Z. Zhu, G. Shan, S.Z. Luo, A direct determination of AFBs in vinegar by aptamer-based surface plasmon resonance biosensor, Toxicon (2018), https://doi.org/10.1016/j.toxicon.2018.03.006.
[95] L. Sun, L. Wu, Q. Zhao, Aptamer based surface plasmon resonance sensor for aflatoxin B1, Microchim. Acta (2017), https://doi.org/10.1007/s00604-017-2265-5.
[96] Y. Zhao, Y. Yang, Y. Luo, X. Yang, M. Li, Q. Song, Double detection of mycotoxins based on SERS labels embedded Ag@Au core-shell nanoparticles, ACS Appl. Mater. Interfaces (2015), https://doi.org/10.1021/acsami.5b07804.
[97] M. Yang, G. Liu, H.M. Mehedi, Q. Ouyang, Q. Chen, A universal SERS aptasensor based on DTNB labeled GNTs/Ag core-shell nanotriangle and CS-Fe3O4 magnetic-bead trace detection of Aflatoxin B1, Anal. Chim. Acta (2017).
[98] A.K. Sharma, M.S. Gaur, P. Sharma, R.K. Tiwari, S. Bhadoria, Development of colorimetric sensor instrument for quantitative analysis of methyl parathion, Sens, Rev (2009), https://doi.org/10.1108/02602280910926779.
[99] M. Jafari, M. Rezaei, H. Kalantari, M. Tabarzad, B. Daraei, Optimization of aflatoxin B1 aptasensing, J. Toxicol. (2017), https://doi.org/10.1155/2017/2461354.
[100] A. Chen, S. Yang, Replacing antibodies with aptamers in lateral flow immunoassay, Biosens, Bioelectron (2015), https://doi.org/10.1016/j.bios.2015.04.041.
[101] S. Mackay, D. Wishart, J.Z. Xing, J. Chen, Developing trends in aptamer-based biosensor devices and their applications, IEEE Trans. Biomed. Circuits Syst. https://doi.org/10.1109/TBCAS.2014.2304718, 2014.
[102] S.M. Bone, N.E. Lima, A.V. Todd, DNAzyme switches for molecular computation and signal amplification, Biosens, Bioelectron (2015), https://doi.org/10.1016/j.bios.2015.03.057.
[103] M. Jafari, M. Rezaei, H. Kalantari, M. Tabarzad, B. Daraei, DNAzyme–aptamer or aptamer–DNAzyme paradigm: biochemical approach for aflatoxin analysis, Biotechnol. Appl. Biochem. (2018), https://doi.org/10.1002/bab.1563.
[104] Y. Seok, J.Y. Byun, W.B. Shim, M.G. Kim, A structure-switchable aptasensor for aflatoxin B1 detection based on assembly of an aptamer/split DNAzyme, Anal. Chim. Acta (2015), https://doi.org/10.1016/j.aca.2015.05.041.
[105] W.B. Shim, H. Mun, H.A. Joung, J.A. Ofori, D.H. Chung, M.G. Kim, Chemiluminescence competitive aptamer assay for the detection of aflatoxin B1 in corn samples, Food Contr. (2014), https://doi.org/10.1016/j.foodcont.2013.07.042.
[106] L. Sun, Q. Zhao, Competitive horseradish peroxidase-linked aptamer assay for sensitive detection of Aflatoxin B1, Talanta (2018), https://doi.org/10.1016/j.talanta.2017.11.048.
[107] M. Joo, S.H. Baek, S.A. Cheon, H.S. Chun, S.W. Choi, T.J. Park, Development of aflatoxin B1 aptasensor based on wide-range fluorescence detection using graphene oxide quencher, Colloids Surfaces B Biointerfaces. https://doi.org/10.1016/j.colsurfb.2017.03.010, 2017.
[108] J. Zhang, Z. Li, S. Zhao, Y. Lu, Size-dependent modulation of graphene oxide-aptamer interactions for an amplified fluorescence-based detection of aflatoxin B1with a tunable dynamic range, Analyst (2016), https://doi.org/10.1039/c6an00368k.
[109] B. Wang, Y. Chen, Y. Wu, B. Weng, Y. Liu, Z. Lu, C.M. Li, C. Yu, Aptamer induced assembly of fluorescent nitrogen-doped carbon dots on gold nanoparticles for sensitive detection of AFB1, Biosens. Bioelectron. (2016), https://doi.org/10.1016/j.bios.2015.11.015.
[110] Z. Lu, X. Chen, Y. Wang, X. Zheng, C.M. Li, Aptamer based fluorescence recovery assay for aflatoxin B1 using a quencher system composed of quantum dots and graphene oxide, Microchim, Acta (2014), https://doi.org/10.1007/s00604-014-1360-0.
[111] L. Chen, F. Wen, M. Li, X. Guo, S. Li, N. Zheng, J. Wang, A simple aptamer-based fluorescent assay for the detection of Aflatoxin B1in infant rice cereal, Food Chem. (2017), https://doi.org/10.1016/j.foodchem.2016.07.148.
[112] F.S. Sabet, M. Hosseini, H. Khabbaz, M. Dadmehr, M.R. Ganjali, FRET-based aptamer biosensor for selective and sensitive detection of aflatoxin B1 in peanut and rice, Food Chem. (2017), https://doi.org/10.1016/j.foodchem.2016.10.004.
[113] K.Y. Goud, A. Sharma, A. Hayat, G. Catanante, K.V. Gobi, A.M. Gurban, J. L. Marty, Tetramethyl-6-carboxyrhodamine quenching-based aptasensing platform for aflatoxin B1: analytical performance comparison of two aptamers, Anal. Biochem. (2016), https://doi.org/10.1016/j.ab.2016.05.018.
[114] H. Liu, A. Lu, H. Fu, B. Li, M. Yang, J. Wang, Y. Luan, Affinity capture of aflatoxin B1 and B2 by aptamer-functionalized magnetic agarose microspheres prior to their determination by HPLC, Microchim. Acta (2018), https://doi.org/10.1007/s00604-018-2849-8.
[115] J. Hu, S.Q. Wang, L. Wang, F. Li, B. Pingguan-Murphy, T.J. Lu, F. Xu, Advances in paper-based point-of-care diagnostics, Biosens, Bioelectron (2014), https://doi.org/10.1016/j.bios.2013.10.075.
[116] S. Zhang, S. Zhao, S. Wang, J. Liu, Y. Dong, Development of lateral flow immunochromatographic strips for micropollutant screening using colorants of aptamer-functionalized nanogold particles, Part II: experimental verification with aflatoxin B1 and chloramphenicol, J. AOAC Int. (2018), https://doi.org/10.5740/jaoacint.18-0056.
[117] W.B. Shim, M.J. Kim, H. Mun, M.G. Kim, An aptamer-based dipstick assay for the rapid and simple detection of aflatoxin B1, Biosens. Bioelectron. (2014), https://doi.org/10.1016/j.bios.2014.06.059.
[118] M.A. Klich, Soil fungi of some low-altitude desert cotton fields and ability of their extracts to inhibit Aspergillus flavus, Mycopathologia (1998), https://doi.org/10.1023/A:1006989712282.
[119] M.O. Moss, Recent studies of mycotoxins, J. Appl. Microbiol. Symp. Suppl (1998).
[120] A.D. Sweeney, J. M, Dobson, Mycotoxin production by Aspergillus, Fusarium and Penicillium species, Int. J. Food Microbiol. (1998).
[121] P.D. Andrade, J.L.G. da Silva, E.D. Caldas, Simultaneous analysis of aflatoxins B1, B2, G1, G2, M1 and ochratoxin A in breast milk by high-performance liquid chromatography/fluorescence after liquid-liquid extraction with low temperature purification (LLE-LTP), J. Chromatogr. A (2013), https://doi.org/10.1016/j.chroma.2013.06.049.
[122] Y. Jiang, P.E. Jolly, W.O. Ellis, J.S. Wang, T.D. Phillips, J.H. Williams, Aflatoxin B1 albumin adduct levels and cellular immune status in Ghanaians, Int, Immunol. (2005), https://doi.org/10.1093/intimm/dxh262.

[123] T.W. Kensler, B.D. Roebuck, G.N. Wogan, J.D. Groopman, Aflatoxin: a 50-year Odyssey of mechanistic and translational toxicology, Toxicol, Sci (2011), https://doi.org/10.1093/toxsci/kfq283.
[124] G.N. Wogan, T.W. Kensler, J.D. Groopman, Present and future directions of translational research on aflatoxin and hepatocellular carcinoma. A review., Food Addit. Contam. Part A. Chem. Anal. Control. Expo, Risk Assess (2012), https://doi.org/10.1080/19440049.2011.563370.
[125] V. Hodnik, G. Anderluh, Toxin detection by surface plasmon resonance, Sensors (2009), https://doi.org/10.3390/s9031339.
[126] E.N. Ediage, J.D. Di Mavungu, S. Monbaliu, C. Van Peteghem, S. De Saeger, A validated multianalyte LC-MS/MS method for quantification of 25 mycotoxins in cassava flour, peanut cake and maize samples, J. Agric. Food Chem. (2011), https://doi.org/10.1021/jf2009364.
[127] X.W. Lai, D.L. Sun, C.Q. Ruan, H. Zhang, C.L. Liu, Rapid analysis of aflatoxins B1, B2, and ochratoxin A in rice samples using dispersive liquid-liquid microextraction combined with HPLC, J. Separ. Sci. (2014), https://doi.org/10.1002/jssc.201300970.
[128] A.S. Luna, R.A. Luiz, I.C.A. Lima, P.H. Março, P. Valderrama, R. Boqué, J. Ferré, Simultaneous determination of aflatoxins B2 and G2 in peanuts using spectrofluorescence coupled with parallel factor analysis, Anal. Chim, Acta (2013), https://doi.org/10.1016/j.aca.2013.03.038.
[129] L. Abrunhosa, H. Morales, C. Soares, T. Calado, A.S. Vila-Chã, M. Pereira, A. Venâncio, A review of mycotoxins in food and feed products in Portugal and estimation of probable daily intakes, Crit. Rev. Food Sci. Nutr. (2016), https://doi.org/10.1080/10408398.2012.720619.
[130] L.F. McCoy, P.F. Scholl, A.E. Sutcliffe, S.M. Kieszak, C.D. Powers, H.S. Rogers, Y. Y. Gong, J.D. Groopman, C.P. Wild, R.L. Schleicher, Human aflatoxin albumin adducts quantitatively compared by ELISA, HPLC with fluorescence detection, and HPLC with isotope dilution mass spectrometry, Cancer Epidemiol. Biomark. Prev. (2008), https://doi.org/10.1158/1055-9965.EPI-07-2780.
[131] N.A. Lee, S. Wang, R.D. Allan, I.R. Kennedy, A rapid aflatoxin B1 ELISA: development and validation with reduced matrix effects for peanuts, Corn, Pistachio, and Soybeans, J. Agric. Food Chem (2004), https://doi.org/10.1021/jf0354038.
[132] D. Moscone, F. Arduini, A. Amine, A rapid enzymatic method for aflatoxin B detection, Methods Mol. Biol. (2011), https://doi.org/10.1007/978-1-61779-102-4_20.
[133] Y. Luan, J. Chen, G. Xie, C. Li, H. Ping, Z. Ma, A. Lu, Visual and microplate detection of aflatoxin B2 based on NaCl-induced aggregation of aptamer-modified gold nanoparticles, Microchim, Acta (2015), https://doi.org/10.1007/s00604-014-1420-5.
[134] W. Xu, Y. Qing, S. Chen, J. Chen, Z. Qin, J.F. Qiu, C.R. Li, Electrochemical indirect competitive immunoassay for ultrasensitive detection of zearalenone based on a glassy carbon electrode modified with carboxylated multi-walled carbon nanotubes and chitosan, Microchim, Acta (2017), https://doi.org/10.1007/s00604-017-2342-9.
[135] L. Liu, Y. Chao, W. Cao, Y. Wang, C. Luo, X. Pang, D. Fan, Q. Wei, A label-free amperometric immunosensor for detection of zearalenone based on trimetallic Au-core/AgPt-shell nanorattles and mesoporous carbon, Anal. Chim. Acta (2014), https://doi.org/10.1016/j.aca.2014.07.026.
[136] H. Riberi, W.I. Tarditto, L.V. Zon, M.A. Arevalo, F.J. Fernandez, Development of an electrochemical immunosensor to determine zearalenone in maize using carbon screen printed electrodes modified with multi-walled carbon nanotubes/polyethyleneimine dispersions, Sens, Actuators (2018).
[137] B. Jarošová, J. Javůrek, O. Adamovský, K. Hilscherová, Phytoestrogens and mycoestrogens in surface waters - their sources, occurrence, and potential contribution to estrogenic activity, Environ, Bar Int. (2015), https://doi.org/10.1016/j.envint.2015.03.019.
[138] P. Schwartz, K.L. Thorpe, T.D. Bucheli, F.E. Wettstein, P. Burkhardt-Holm, Short-term exposure to the environmentally relevant estrogenic mycotoxin zearalenone impairs reproduction in fish, Sci. Total Environ. (2010), https://doi.org/10.1016/j.scitotenv.2010.10.017.
[139] P. Majerus, N. Graf, M. Krämer, Rapid determination of zearalenone in edible oils by HPLC with fluorescence detection, Mycotoxin Res. (2009), https://doi.org/10.1007/s12550-009-0018-y.
[140] V.H. Pallaroni L, E. Bjorklund, Optimization of atmospheric pressure chemical ionization interface parameters for the simultaneous determination of deoxynivalenol and zearalenone using HPLC/MS, Liq Chromatogr Relat Technol 25 (2002).
[141] S. Biselli, H. Wegner, C. Hummert, A multicomponent method for Fusarium toxins in cereal based food and feed samples using HPLC-MS/MS, in: Mycotoxin Res, 2005, https://doi.org/10.1007/BF02954808.
[142] N.A. Burmistrova, I.Y. Goryacheva, E.Y. Basova, A.S. Franki, D. Elewaut, K. Van Beneden, D. Deforce, C. Van Peteghem, S. De Saeger, Application of a new anti-zearalenone monoclonal antibody in different immunoassay formats, Anal. Bioanal, Inside Chem. (2009), https://doi.org/10.1007/s00216-009-2913-7.
[143] W.B. Shim, B.B. Dzantiev, S.A. Eremin, D.H. Chung, One-step simultaneous immunochromatographic strip test for multianalysis of ochratoxin A and Zearalenone, J. Microbiol. Biotechnol. (2009), https://doi.org/10.4014/jmb.0802.105.
[144] H.S. Chun, E.H. Choi, H.J. Chang, S.W. Choi, S.A. Eremin, A fluorescence polarization immunoassay for the detection of zearalenone in corn, Anal. Chim. Acta (2009), https://doi.org/10.1016/j.aca.2009.02.048.
[145] J. Jantra, K. Zór, M. Sanders, S. De Saeger, M. Hedström, B. Mattiasson, Development of an automated flow-based spectrophotometric immunoassay for continuous detection of zearalenone, Biotechnol. Appl. Biochem. (2019), https://doi.org/10.1002/bab.1876.
[146] X. Chen, Y. Huang, N. Duan, S. Wu, X. Ma, Y. Xia, C. Zhu, Y. Jiang, Z. Wang, Selection and identification of ssDNA aptamers recognizing zearalenone, Anal. Bioanal. Chem. (2013), https://doi.org/10.1007/s00216-013-7085-9.
[147] K. Abnous, N.M. Danesh, M. Ramezani, A.S. Emrani, S.M. Taghdisi, A novel colorimetric sandwich aptasensor based on an indirect competitive enzyme-free method for ultrasensitive detection of chloramphenicol, Biosens. Bioelectron. (2016), https://doi.org/10.1016/j.bios.2015.11.028.
[148] Z. Gao, Z. Qiu, M. Lu, J. Shu, D. Tang, Hybridization chain reaction-based colorimetric aptasensor of adenosine 5′-triphosphate on unmodified gold nanoparticles and two label-free hairpin probes, Biosens. Bioelectron. (2017), https://doi.org/10.1016/j.bios.2016.10.043.
[149] Khalil A. Seyed Mohammad Taghdisi, Noor Mohammad Danesh, Parirokh Lavaee, de Ahmad Sarreshtehdar Emrani, Mohammad Ramezani, A novel colorimetric triple-helix molecular switch aptasensor based on peroxidase-like activity of gold nanoparticles for ultrasensitive detection of lead(II), RSC Adv. (2015).
[150] Y. Mao, T. Fan, R. Gysbers, Y. Tan, F. Liu, S. Lin, Y. Jiang, A simple and sensitive aptasensor for colorimetric detection of adenosine triphosphate based on unmodified gold nanoparticles, Talanta (2017), https://doi.org/10.1016/j.talanta.2017.03.014.
[151] Z. Chen, L. Tan, L. Hu, Y. Zhang, S. Wang, F. Lv, Real colorimetric thrombin aptasensor by masking surfaces of catalytically active gold nanoparticles, ACS Appl. Mater. Interfaces (2016), https://doi.org/10.1021/acsami.5b08975.
[152] S.M. Taghdisi, N.M. Danesh, M. Ramezani, A.S. Emrani, K. Abnous, Novel colorimetric aptasensor for zearalenone detection based on nontarget-induced aptamer walker, gold nanoparticles, and exonuclease-assisted recycling amplification, ACS Appl. Mater. Interfaces (2018), https://doi.org/10.1021/acsami.8b02349.
[153] Z. Wu, E. Xu, M.F.J. Chughtai, Z. Jin, J. Irudayaraj, Highly sensitive fluorescence sensing of zearalenone using a novel aptasensor based on upconverting nanoparticles, Food Chem. (2017), https://doi.org/10.1016/j.foodchem.2017.03.100.
[154] Z. Li, Y. Zhang, An efficient and user-friendly method for the synthesis of hexagonal-phase NaYF4:Yb, Er/Tm nanocrystals with controllable shape and upconversion fluorescence, Nanotechnology (2008), https://doi.org/10.1088/0957-4484/19/34/345606.
[155] W. Stöber, A. Fink, E. Bohn, Controlled growth of monodisperse silica spheres in the micron size range, J. Colloid Interface Sci. (1968) 90272–90275, https://doi.org/10.1016/0021-9797(68.
[156] L. Chen, J. Liu, Q. Zeng, H. Wang, A. Yu, H. Zhang, L. Ding, Preparation of magnetic molecularly imprinted polymer for the separation of tetracycline antibiotics from egg and tissue samples, J. Chromatogr. A (2009), https://doi.org/10.1016/j.chroma.2009.02.044.
[157] B. Zhang, Y. Pan, H. Chen, T. Liu, H. Tao, Y. Tian, Stabilization of starch-based microgel-lysozyme complexes using a layer-by-layer assembly technique, Food Chem. (2017), https://doi.org/10.1016/j.foodchem.2016.07.076.
[158] X. Hu, L. Mu, J. Wen, Q. Zhou, Covalently synthesized graphene oxide-aptamer nanosheets for efficient visible-light photocatalysis of nucleic acids and proteins of viruses, Carbon N. Y (2012), https://doi.org/10.1016/j.carbon.2012.02.038.
[159] R. Cai, W. Rao, Z. Zhang, F. Long, Y. Yin, An imprinted electrochemical sensor for bisphenol A determination based on electrodeposition of a graphene and Ag nanoparticle modified carbon electrode, Anal, Methods (2014), https://doi.org/10.1039/c3ay42125b.
[160] K. Yugender Goud, A. Hayat, M. Satyanarayana, V. Sunil Kumar, G. Catanante, K. Vengatajalabathy Gobi, J.L. Marty, Aptamer-based zearalenone assay based on the use of a fluorescein label and a functional graphene oxide as a quencher, Microchim. Acta (2017), https://doi.org/10.1007/s00604-017-2487-6.
[161] L. Wang, J. Bao, L. Wang, F. Zhang, Y. Li, One-pot synthesis and bioapplication of amine-functionalized magnetite nanoparticles and hollow nanospheres, Chem. Eur J. (2006), https://doi.org/10.1002/chem.200501334.
[162] D. Tu, L. Liu, Q. Ju, Y. Liu, H. Zhu, R. Li, X. Chen, Time-resolved FRET biosensor based on amine-functionalized lanthanide-doped NaYF4 nanocrystals, Angew. Chemie - Int (2011), https://doi.org/10.1002/anie.201100303.
[163] Y. Huang, H. Zhang, X. Chen, X. Wang, N. Duan, S. Wu, B. Xu, Z. Wang, A multicolor time-resolved fluorescence aptasensor for the simultaneous detection of multiplex Staphylococcus aureus enterotoxins in the milk, Biosens. Bioelectron. (2015), https://doi.org/10.1016/j.bios.2015.06.046.
[164] S. Niazi, X. Wang, I. Pasha, I.M. Khan, S. Zhao, M. Shoaib, S. Wu, Z. Wang, A novel bioassay based on aptamer-functionalized magnetic nanoparticle for the detection of zearalenone using time resolved-fluorescence NaYF4: Ce/Tb nanoparticles as signal probe, Talanta (2018), https://doi.org/10.1016/j.talanta.2018.04.013.
[165] S. Niazi, I.M. Khan, Y. Yu, I. Pasha, M. Shoaib, A. Mohsin, B.S. Mushtaq, W. Akhtar, Z. Wang, A “turnon” aptasensor for simultaneous and time-resolved fluorometric determination of zearalenone, trichothecenes A and aflatoxin B1 using WS2 as a quencher, Microchim, Acta (2019), https://doi.org/10.1007/s00604-019-3570-y.
[166] Z. Han, Z. Tang, K. Jiang, Q. Huang, J. Meng, D. Nie, Z. Zhao, Dual-target electrochemical aptasensor based on co-reduced molybdenum disulfide and Au NPs (rMoS2-Au) for multiplex detection of mycotoxins, Biosens, Bioelectron (2020), https://doi.org/10.1016/j.bios.2019.111894.
[167] X. Ji, C. Yu, Y. Wen, J. Chen, Y. Yu, C. Zhang, R. Gao, X. Mu, J. He, Fabrication of pioneering 3D sakura-shaped metal-organic coordination polymers Cu@L-Glu phenomenal for signal amplification in highly sensitive detection of zearalenone, Biosens. Bioelectron. (2019), https://doi.org/10.1016/j.bios.2019.01.012.

[168] S. Wu, L. Liu, N. Duan, Q. Li, Y. Zhou, Z. Wang, Aptamer-based lateral flow test strip for rapid detection of zearalenone in corn samples, J. Agric. Food Chem. (2018), https://doi.org/10.1021/acs.jafc.7b05326.
[169] A. Visconti, M.B. Doko, M. Solfrizzo, M. Pascale, A. Boenke, European intercomparison study for the determination of fumonisins in maize, mikrochim, Acta (1996), https://doi.org/10.1007/BF01244378.
[170] C.D. Muscarella M, S.L. Magroa, D. Nardiello, C. Palermo, Development of a new analytical method for the determination of fumonisins B1 and B2 in food products based on high performance liquid chromatography and fluorimetric detection with post-column derivatization, J. Chromatogr. A (2008).
[171] M. McKeague, C.R. Bradley, A. de Girolamo, A. Visconti, J. David Miller, M.C. de Rosa, Screening and initial binding assessment of fumonisin B1aptamers, Int. J. Mol. Sci. (2010), https://doi.org/10.3390/ijms11124864.
[172] M. Wang, G. Abbineni, A. Clevenger, C. Mao, S. Xu, Upconversion nanoparticles: synthesis, surface modification and biological applications, Nanomed. Nanotechnol. Biol. Med. (2011), https://doi.org/10.1016/j.nano.2011.02.013.
[173] S. Wu, N. Duan, X. Ma, Y. Xia, H. Wang, Z. Wang, Q. Zhang, Multiplexed fluorescence resonance energy transfer aptasensor between upconversion nanoparticles and graphene oxide for the simultaneous determination of mycotoxins, Anal. Chem. (2012), https://doi.org/10.1021/ac301534w.
[174] R.M. Clegg, The vital contribution of perrin and forster, Biophot. Int. 11 (2004) 42–44. Biophotonics Int. 11, 42–44. (2004).
[175] D. He, Z. Wu, B. Cui, E. Xu, Aptamer and gold nanorod–based fumonisin B1 assay using both fluorometry and SERS, Microchim. Acta (2020), https://doi.org/10.1007/s00604-020-4192-0.
[176] C. Wang, X. Huang, X. Tian, X. Zhang, S. Yu, X. Chang, Y. Ren, J. Qian, A multiplexed FRET aptasensor for the simultaneous detection of mycotoxins with magnetically controlled graphene oxide/Fe3O4 as a single energy acceptor, Analyst (2019), https://doi.org/10.1039/c9an01593k.
[177] S. Niazi, I.M. Khan, L. Yan, M.I. Khan, A. Mohsin, N. Duan, S. Wu, Z. Wang, Simultaneous detection of fumonisin B 1 and ochratoxin A using dual-color, time-resolved luminescent nanoparticles (NaYF 4 : Ce, Tb and NH 2 -Eu/DPA@SiO 2) as labels, Anal. Bioanal. Chem. (2019), https://doi.org/10.1007/s00216-019-01580-0.
[178] S. Yue, X. Jie, L. Wei, C. Bin, W. Dou Dou, Y. Yi, L. Qingxia, L. Jianlin, Z. Tiesong, Simultaneous detection of ochratoxin a and fumonisin b1 in cereal samples using an aptamer-photonic crystal encoded suspension array, Anal, Inside Chem. (2014), https://doi.org/10.1021/ac503355n.
[179] A. Chrouda, A. Sbartai, A. Baraket, L. Renaud, A. Maaref, N. Jaffrezic-Renault, An aptasensor for ochratoxin A based on grafting of polyethylene glycol on a boron-doped diamond microcell, Anal, Biochem (2015), https://doi.org/10.1016/j.ab.2015.07.012.
[180] A.E. el Khoury, A. Atoui, Ochratoxin a: general overview and actual molecular status, Toxins, Basel, 2010, https://doi.org/10.3390/toxins2040461.
[181] C. Wang, X. Dong, Q. Liu, K. Wang, Label-free colorimetric aptasensor for sensitive detection of ochratoxin A utilizing hybridization chain reaction, Anal. Chim, Acta (2015), https://doi.org/10.1016/j.aca.2014.12.031.
[182] J. Huang, L. Zheng, N. Zheng, B. Wen, F. Cheng, J. Han, R. Xu, X. Li, S. Wang, Simultaneous determination of aflatoxin M 1, ochratoxin A, zearalenone and α-zearalenol in milk by UHPLC–MS/MS, Food Chem. (2014).
[183] R. Roland, A. Bros, P. Bouisseau, A. Cavelier, F. Schneider, Analysis of ochratoxin A in grapes, musts and wines by LC–MS/MS: first comparison of stable isotope dilution assay and diastereomeric dilution assay methods, Anal. Chem. (2014).
[184] L. Pussemier, J.-Y. Piérard, M. Anselme, E.K. Tangni, J.-C. Motte, Y. Larondelle, Development and application of analytical methods for the determination of mycotoxins in organic and conventional wheat, Food Addit, Contam (2006), https://doi.org/10.1080/02652030600699312.
[185] M. Venkataramana, R. Rashmi, S.R. Uppalapati, S. Chandranayaka, K. Balakrishna, M. Radhika, V.K. Gupta, H.V. Batra, Development of sandwich dot-ELISA for specific detection of Ochratoxin A and its application on to contaminated cereal grains originating from India, Front, Microbiol. (2015), https://doi.org/10.3389/fmicb.2015.00511.
[186] C. Wang, J. Qian, K. Wang, K. Wang, Q. Liu, X. Dong, C. Wang, X. Huang, Magnetic-fluorescent-targeting multifunctional aptasensorfor highly sensitive and one-step rapid detection of ochratoxin A, Biosens. Bioelectron. (2015), https://doi.org/10.1016/j.bios.2015.02.008.
[187] J.A. Cruz-Aguado, G. Penner, Determination of ochratoxin A with a DNA aptamerCruz-Aguado, J. Agric. Food Chem. (2008). https://doi.org/10.1021/jf801957h.
[188] H. Badie Bostan, N.M. Danesh, G. Karimi, M. Ramezani, S.A. Mousavi Shaegh, K. Youssefi, F. Charbgoo, K. Abnous, S.M. Taghdisi, Ultrasensitive detection of ochratoxin A using aptasensors, Biosens, Bioelectron (2017), https://doi.org/10.1016/j.bios.2017.06.055.
[189] J. Xu, X. Qiao, Y. Wang, Q. Sheng, T. Yue, J. Zheng, M. Zhou, Electrostatic assembly of gold nanoparticles on black phosphorus nanosheets for electrochemical aptasensing of patulin, Microchim, Acta (2019), https://doi.org/10.1007/s00604-019-3339-3.
[190] W. YuanKai, Z. Qi, S. JianHe, W. HengAn, S. XingMin, C. ZhiFei, Y. YaXian, Screening of single-Stranded DNA (ssDNA) aptamers against a zearalenone monoclonal antibody and development of a ssDNA-based enzyme-linked oligonucleotide assay for determination of zearalenone in corn, J. Agric. Food Chem. (2015).
[191] Y. Zhang, T. Lu, Y. Wang, C. Diao, Y. Zhou, L. Zhao, H. Chen, Selection of a DNA aptamer against zearalenone and docking analysis for highly sensitive rapid visual detection with label-free aptasensor, J. Agric. Food Chem. (2018), https://doi.org/10.1021/acs.jafc.8b03963.
[192] L. Luo, S. Ma, L. Li, X. Liu, J. Zhang, X. Li, D. Liu, T. You, Monitoring zearalenone in corn flour utilizing novel self-enhanced electrochemiluminescence aptasensor based on NGQDs-NH 2 -Ru@SiO 2 luminophore, Food Chem. (2019), https://doi.org/10.1016/j.foodchem.2019.04.050.
[193] Z. Mu, L. Ma, J. Wang, J. Zhou, Y. Yuan, L. Bai, A target-induced amperometic aptasensor for sensitive zearalenone detection by CS@AB-MWCNTs nanocomposite as enhancers, Food Chem. (2021), https://doi.org/10.1016/j.foodchem.2020.128128.
[194] H. Tan, T. Guo, H. Zhou, H. Dai, Y. Yu, H. Zhu, H. Wang, Y. Fu, Y. Zhang, L. Ma, A simple mesoporous silica nanoparticle-based fluorescence aptasensor for the detection of zearalenone in grain and cereal products, Anal. Bioanal. Chem. (2020), https://doi.org/10.1007/s00216-020-02778-3.
[195] Z. Wu, D. He, B. Cui, Z. Jin, E. Xu, C. Yuan, P. Liu, Y. Fang, Q. Chai, Trimer-based aptasensor for simultaneous determination of multiple mycotoxins using SERS and fluorimetry, Microchim, Acta (2020), https://doi.org/10.1007/s00604-020-04487-1.
[196] Á. Molinero-Fernández, A. Jodra, M. Moreno-Guzmán, M.Á. López, A. Escarpa, Cover feature: magnetic reduced graphene oxide/nickel/platinum nanoparticles micromotors for mycotoxin analysis, Chem. Eur J. (2018), https://doi.org/10.1002/chem.201801524.
[197] Á. Molinero-Fernández, M. Moreno-Guzmán, M.Á. López, A. Escarpa, Biosensing strategy for simultaneous and accurate quantitative analysis of mycotoxins in food samples using unmodified graphene micromotors, anal, Inside Chem. (2017), https://doi.org/10.1021/acs.analchem.7b02440.
[198] S. Niazi, I.M. Khan, L. Yan, M.I. Khan, A. Mohsin, N. Duan, S. Wu, Z. Wang, Simultaneous detection of fumonisin B 1 and ochratoxin A using dual-color, time-resolved luminescent nanoparticles (NaYF 4 : Ce, Tb and NH 2 -Eu/DPA@SiO 2) as labels, Anal. Bioanal. Chem. (2019), https://doi.org/10.1007/s00216-019-01580-0.
[199] J. Qian, C. Ren, C. Wang, W. Chen, X. Lu, H. Li, Q. Liu, N. Hao, H. Li, K. Wang, Magnetically controlled fluorescence aptasensor for simultaneous determination of ochratoxin A and aflatoxin B1, Anal. Chim. Acta (2018), https://doi.org/10.1016/j.aca.2018.02.063.
[200] J. Zhang, Y.K. Xia, M. Chen, D.Z. Wu, S.X. Cai, M.M. Liu, W.H. He, J.H. Chen, A fluorescent aptasensor based on DNA-scaffolded silver nanoclusters coupling with Zn(II)-ion signal-enhancement for simultaneous detection of OTA and AFB1, Sensor. Actuator. B Chem. (2016), https://doi.org/10.1016/j.snb.2016.05.061.
[201] Y. Li, J. Wang, B. Zhang, Y. He, J. Wang, S. Wang, A rapid fluorometric method for determination of aflatoxin B 1 in plant-derived food by using a thioflavin T-based aptasensor, Microchim. Acta (2019), https://doi.org/10.1007/s00604-019-3325-9.
[202] X. Lu, C. Wang, J. Qian, C. Ren, K. An, K. Wang, Target-driven switch-on fluorescence aptasensor for trace aflatoxin B1 determination based on highly fluorescent ternary CdZnTe quantum dots, Anal. Chim, Acta (2019), https://doi.org/10.1016/j.aca.2018.10.002.
[203] L. Wang, F. Zhu, M. Chen, Y.Q. Zhu, J. Xiao, H. Yang, X. Chen, Rapid and visual detection of aflatoxin B1 in foodstuffs using aptamer/G-quadruplex DNAzyme probe with low background noise, Food Chem. (2019), https://doi.org/10.1016/j.foodchem.2018.08.007.
[204] S.M. Taghdisi, N.M. Danesh, M. Ramezani, K. Abnous, A new amplified fluorescent aptasensor based on hairpin structure of G-quadruplex oligonucleotide-Aptamer chimera and silica nanoparticles for sensitive detection of aflatoxin B 1 in the grape juice, Food Chem. (2018), https://doi.org/10.1016/j.foodchem.2018.06.101.
[205] Q. Chen, M. Yang, X. Yang, H. Li, Z. Guo, M.H. Rahma, A large Raman scattering cross-section molecular embedded SERS aptasensor for ultrasensitive Aflatoxin B1 detection using CS-Fe3O4for signal enrichment, Spectrochim. Acta - Part A Mol. Biomol, Spectroscopy (Glos.) (2018), https://doi.org/10.1016/j.saa.2017.08.029.
[206] Y.V.V.A. Kumar, R.M. Renuka, J. Achuth, M. Venkataramana, M. Ushakiranmayi, P. Sudhakar, Development of hybrid IgG-aptamer sandwich immunoassay platform for aflatoxin B1 detection and its evaluation onto various field samples, Front, Pharmacol (2018), https://doi.org/10.3389/fphar.2018.00271.
[207] X. Ma, W. Wang, X. Chen, Y. Xia, S. Wu, N. Duan, Z. Wang, Selection, identification, and application of Aflatoxin B1 aptamer, Eur. Food Res. Technol. (2014), https://doi.org/10.1007/s00217-014-2176-1.
[208] Y. Jia, F. Wu, P. Liu, G. Zhou, B. Yu, X. Lou, F. Xia, A label-free fluorescent aptasensor for the detection of Aflatoxin B1 in food samples using AIEgens and graphene oxide, Talanta (2019), https://doi.org/10.1016/j.talanta.2019.01.078.
[209] H. Tan, L. Ma, T. Guo, H. Zhou, L. Chen, Y. Zhang, H. Dai, Y. Yu, A novel fluorescence aptasensor based on mesoporous silica nanoparticles for selective and sensitive detection of aflatoxin B 1, Anal. Chim. Acta (2019), https://doi.org/10.1016/j.aca.2019.04.014.
[210] X. Guo, F. Wen, Q. Qiao, N. Zheng, M. Saive, M.L. Fauconnier, J. Wang, A novel graphene oxide-based aptasensor for amplified fluorescent detection of aflatoxin M1 in milk powder, Sensors (2019), https://doi.org/10.3390/s19183840.
[211] B.H. Nguyen, L.D. Tran, Q.P. Do, H. Le Nguyen, N.H. Tran, P.X. Nguyen, Label-free detection of aflatoxin M1 with electrochemical Fe 3O4/polyaniline-based aptasensor, Mater. Sci. Eng. C (2013), https://doi.org/10.1016/j.msec.2013.01.044.
[212] A. Sharma, G. Catanante, A. Hayat, G. Istamboulie, I. Ben Rejeb, S. Bhand, J. L. Marty, Development of structure switching aptamer assay for detection of aflatoxin M1 in milk sample, Talanta (2016), https://doi.org/10.1016/j.talanta.2016.05.043.
[213] G. Istamboulié, N. Paniel, L. Zara, L.R. Granados, L. Barthelmebs, T. Noguer, Development of an impedimetric aptasensor for the determination of aflatoxin M1 in milk, Talanta (2016), https://doi.org/10.1016/j.talanta.2015.09.012.

[214] Y. Tang, X. Liu, H. Zheng, L. Yang, L. Li, S. Zhang, Y. Zhou, S. Alwarappan, A photoelectrochemical aptasensor for aflatoxin B1 detection based on an energy transfer strategy between Ce-TiO 2 @MoSe 2 and Au nanoparticles, Nanoscale (2019), https://doi.org/10.1039/c9nr01960j.

[215] C. Wang, J. Qian, K. An, X. Lu, X. Huang, A semiconductor quantum dot-based ratiometric electrochemical aptasensor for the selective and reliable determination of aflatoxin B1, Analyst (2019), https://doi.org/10.1039/c9an00825j.

[216] A. Beheshti-Marnani, A. Hatefi-Mehrjardi, Z. Es'haghi, A sensitive biosensing method for detecting of ultra-trace amounts of AFB1 based on "Aptamer/reduced graphene oxide" nano-bio interaction, Colloids Surf. B Biointerfaces (2019), https://doi.org/10.1016/j.colsurfb.2018.11.087.

[217] C. Wang, Y. Li, Q. Zhao, A signal-on electrochemical aptasensor for rapid detection of aflatoxin B1 based on competition with complementary DNA, Biosens. Bioelectron. (2019), https://doi.org/10.1016/j.bios.2019.111641.

[218] Y. Yao, H. Wang, X. Wang, X. Wang, F. Li, Development of a chemiluminescent aptasensor for ultrasensitive and selective detection of aflatoxin B1 in peanut and milk, Talanta (2019), https://doi.org/10.1016/j.talanta.2019.03.109.

[219] S.S. Wu, M. Wei, W. Wei, Y. Liu, S. Liu, Electrochemical aptasensor for aflatoxin B1 based on smart host-guest recognition of β-cyclodextrin polymer, Biosens. Bioelectron. (2019), https://doi.org/10.1016/j.bios.2019.01.022.

[220] G. Selvolini, M. Lettieri, L. Tassoni, S. Gastaldello, M. Grillo, C. Maran, G. Marrazza, Electrochemical enzyme-linked oligonucleotide array for aflatoxin B1 detection, Talanta (2019), https://doi.org/10.1016/j.talanta.2019.05.044.

[221] B. Wang, J. Zheng, A. Ding, L. Xu, J. Chen, C.M. Li, Highly sensitive aflatoxin B1 sensor based on DNA-guided assembly of fluorescent probe and TdT-assisted DNA polymerization, Food Chem. (2019), https://doi.org/10.1016/j.foodchem.2019.05.025.

[222] X. Yang, D. Shi, S. Zhu, B. Wang, X. Zhang, G. Wang, Portable Aptasensor of aflatoxin B1 in bread based on a personal glucose meter and DNA walking machine, ACS Sens. (2018), https://doi.org/10.1021/acssensors.8b00304.

[223] Y. Li, D. Liu, C. Zhu, X. Shen, Y. Liu, T. You, Sensitivity programmable ratiometric electrochemical aptasensor based on signal engineering for the detection of aflatoxin B1 in peanut, J. Hazard Mater. (2020), https://doi.org/10.1016/j.jhazmat.2019.122001.

[224] B. Zhang, Y. Lu, C. Yang, Q. Guo, G. Nie, Simple "signal-on" photoelectrochemical aptasensor for ultrasensitive detecting AFB1 based on electrochemically reduced graphene oxide/poly(5-formylindole)/Au nanocomposites, Biosens, Bioelectron (2019), https://doi.org/10.1016/j.bios.2019.03.048.

[225] C. Gu, L. Yang, M. Wang, N. Zhou, L. He, Z. Zhang, M. Du, A bimetallic (Cu-Co) Prussian Blue analogue loaded with gold nanoparticles for impedimetric aptasensing of ochratoxin a, Microchim. Acta (2019), https://doi.org/10.1007/s00604-019-3479-5.

[226] L. Hao, W. Wang, X. Shen, S. Wang, Q. Li, F. An, S. Wu, A fluorescent DNA hydrogel aptasensor based on the self-assembly of rolling circle amplification products for sensitive detection of ochratoxin A, J. Agric. Food Chem. (2020), https://doi.org/10.1021/acs.jafc.9b06021.

[227] D. Song, R. Yang, S. Fang, Y. Liu, F. Long, A FRET-based dual-color evanescent wave optical fiber aptasensor for simultaneous fluorometric determination of aflatoxin M1 and ochratoxin A, Microchim. Acta (2018), https://doi.org/10.1007/s00604-018-3046-5.

[228] Y.-J. Yang, Y. Zhou, Y. Xing, G.-M. Zhang, Y. Zhang, C.-H. Zhang, P. Lei, C. Dong, X. Deng, Y. He, S. Shuang, A Label-free aptasensor based on Aptamer/NH2 Janus particles for ultrasensitive electrochemical detection of Ochratoxin A, Talanta 199 (2019) 310–316, https://doi.org/10.1016/j.talanta.2019.02.015.

[229] F. Tian, J. Zhou, B. Jiao, Y. He, A nanozyme-based cascade colorimetric aptasensor for amplified detection of ochratoxin A, Nanoscale (2019), https://doi.org/10.1039/c9nr02872b.

[230] M. Wei, C. Wang, E. Xu, J. Chen, X. Xu, W. Wei, S. Liu, A simple and sensitive electrochemiluminescence aptasensor for determination of ochratoxin A based on a nicking endonuclease-powered DNA walking machine, Food Chem. (2019), https://doi.org/10.1016/j.foodchem.2019.01.011.

[231] A. Suea-Ngam, P.D. Howes, C.E. Stanley, A.J. Demello, An exonuclease I-assisted silver-metallized electrochemical aptasensor for ochratoxin A detection, ACS Sens. (2019), https://doi.org/10.1021/acssensors.9b00237.

[232] W. Chen, C. Yan, L. Cheng, L. Yao, F. Xue, J. Xu, An ultrasensitive signal-on electrochemical aptasensor for ochratoxin A determination based on DNA controlled layer-by-layer assembly of dual gold nanoparticle conjugates, Biosens, Bioelectron (2018), https://doi.org/10.1016/j.bios.2018.07.012.

[233] J. Gao, Z. Chen, L. Mao, W. Zhang, W. Wen, X. Zhang, S. Wang, Electrochemiluminescent aptasensor based on resonance energy transfer system between CdTe quantum dots and cyanine dyes for the sensitive detection of Ochratoxin A, Talanta (2019), https://doi.org/10.1016/j.talanta.2019.02.044.

[234] C. Ma, K. Wu, H. Zhao, H. Liu, K. Wang, K. Xia, Fluorometric aptamer-based determination of ochratoxin A based on the use of graphene oxide and RNase H-aided amplification, Microchim, Acta (2018), https://doi.org/10.1007/s00604-018-2885-4.

[235] Y. He, F. Tian, J. Zhou, B. Jiao, A fluorescent aptasensor for ochratoxin A detection based on enzymatically generated copper nanoparticles with a polythymine scaffold, Microchim. Acta (2019), https://doi.org/10.1007/s00604-019-3314-z.

[236] D.E. Armstrong-Price, P.S. Deore, R.A. Manderville, Intrinsic "turn-on" aptasensor detection of ochratoxin A using energy-transfer fluorescence, J. Agric. Food Chem. (2020), https://doi.org/10.1021/acs.jafc.9b07391.

[237] L. Liu, Z.I. Tanveer, K. Jiang, Q. Huang, J. Zhang, Y. Wu, Z. Han, Label-free fluorescent aptasensor for ochratoxin—a detection based on CdTe quantum dots and (N-methyl-4-pyridyl) porphyrin, Toxins, Basel, 2019, https://doi.org/10.3390/toxins11080447.

[238] Y. He, F. Tian, J. Zhou, Q. Zhao, R. Fu, B. Jiao, Colorimetric aptasensor for ochratoxin A detection based on enzyme-induced gold nanoparticle aggregation, J. Hazard Mater. (2020), https://doi.org/10.1016/j.jhazmat.2019.121758.

[239] B. Shao, X. Ma, S. Zhao, Y. Lv, X. Hun, H. Wang, Z. Wang, Nanogapped Au(core) @ Au-Ag(shell) structures coupled with Fe3O4 magnetic nanoparticles for the detection of Ochratoxin A, Anal. Chim. Acta (2018), https://doi.org/10.1016/j.aca.2018.05.058.

[240] X. Jing, L. Chang, L. Shi, X. Liu, Y. Zhao, W. Zhang, Au film-Au@Ag core-shell nanoparticle structured surface-enhanced Raman spectroscopy aptasensor for accurate ochratoxin A detection, ACS Appl. Bio Mater (2020), https://doi.org/10.1021/acsabm.0c00120.

[241] M. Nan, Y. Bi, H. Xue, S. Xue, H. Long, L. Pu, G. Fu, Rapid determination of ochratoxin a in grape and its commodities based on a label-free impedimetric aptasensor constructed by layer-by-layer self-assembly, Toxins, Basel, 2019, https://doi.org/10.3390/toxins11020071.

[242] K. Wu, C. Ma, H. Zhao, M. Chen, Z. Deng, Sensitive aptamer-based fluorescene assay for ochratoxin A based on RNase H signal amplification, Food Chem. (2019), https://doi.org/10.1016/j.foodchem.2018.10.130.

[243] P. Wang, L. Wang, M. Ding, M. Pei, W. Guo, Ultrasensitive electrochemical detection of ochratoxin A based on signal amplification by one-pot synthesized flower-like PEDOT-AuNFs supported on a graphene oxide sponge, Analyst (2019), https://doi.org/10.1039/c9an01288e.

[244] B. Han, C. Fang, L. Sha, M. Jalalah, M.S. Al-Assiri, F.A. Harraz, Y. Cao, Cascade strand displacement reaction-assisted aptamer-based highly sensitive detection of ochratoxin A, Food Chem. (2021), https://doi.org/10.1016/j.foodchem.2020.127827.